

**Report on the Physical Properties and
Durability of Fiber-Reinforced Concrete**

Reported by ACI Committee 544



American Concrete Institute®



First Printing
March 2010

American Concrete Institute®
Advancing concrete knowledge

Report on the Physical Properties and Durability of Fiber-Reinforced Concrete

Copyright by the American Concrete Institute, Farmington Hills, MI. All rights reserved. This material may not be reproduced or copied, in whole or part, in any printed, mechanical, electronic, film, or other distribution and storage media, without the written consent of ACI.

The technical committees responsible for ACI committee reports and standards strive to avoid ambiguities, omissions, and errors in these documents. In spite of these efforts, the users of ACI documents occasionally find information or requirements that may be subject to more than one interpretation or may be incomplete or incorrect. Users who have suggestions for the improvement of ACI documents are requested to contact ACI. Proper use of this document includes periodically checking for errata at www.concrete.org/committees/errata.asp for the most up-to-date revisions.

ACI committee documents are intended for the use of individuals who are competent to evaluate the significance and limitations of its content and recommendations and who will accept responsibility for the application of the material it contains. Individuals who use this publication in any way assume all risk and accept total responsibility for the application and use of this information.

All information in this publication is provided “as is” without warranty of any kind, either express or implied, including but not limited to, the implied warranties of merchantability, fitness for a particular purpose or non-infringement.

ACI and its members disclaim liability for damages of any kind, including any special, indirect, incidental, or consequential damages, including without limitation, lost revenues or lost profits, which may result from the use of this publication.

It is the responsibility of the user of this document to establish health and safety practices appropriate to the specific circumstances involved with its use. ACI does not make any representations with regard to health and safety issues and the use of this document. The user must determine the applicability of all regulatory limitations before applying the document and must comply with all applicable laws and regulations, including but not limited to, United States Occupational Safety and Health Administration (OSHA) health and safety standards.

Order information: ACI documents are available in print, by download, on CD-ROM, through electronic subscription, or reprint and may be obtained by contacting ACI.

Most ACI standards and committee reports are gathered together in the annually revised *ACI Manual of Concrete Practice* (MCP).

American Concrete Institute
38800 Country Club Drive
Farmington Hills, MI 48331
U.S.A.

Phone: 248-848-3700
Fax: 248-848-3701

www.concrete.org

ISBN 978-0-87031-365-3

Report on the Physical Properties and Durability of Fiber-Reinforced Concrete

Reported by ACI Committee 544

Nemkumar Banthia
Chair

Neven Krstulovic-Opara
Secretary

Melvyn A. Galinat
Membership Secretary

Ashraf I. Ahmed	Graham T. Gilbert	Pritpal. S. Mangat*	Venkataswamy Ramakrishnan*
Corina-Maria Aldea*	Vellore S. Gopalaratnam	Peter C. Martinez	Roy H. Reiterman
Madasamy Arockiasamy	Antonio J. Guerra	Bruno Massicotte	Klaus Alexander Rieder*
P. N. Balaguru	Rishi Gupta	James R. McConaghy	Pierre Rossi
Joaquim Oliveira Barros*	Carol D. Hays	Christian Meyer	Surendra P. Shah
Gordon B. Batson*	George C. Hoff	Nicholas C. Mitchell Jr.	Konstantin Sobolev
Vivek S. Bindiganavile	Allen J. Hulshizer	Barzin Mobasher†	Jim D. Speakman Sr.
Peter H. Bischoff	Akm Anwarul Islam	Henry J. Molloy	Chris D. Szychowski
Marvin E. Criswell	John Jones*	Dudley R. Morgan	Peter C. Tatnall
James I. Daniel	Jubum Kim	Antoine E. Naaman*	Houssam A. Toutanji
Xavier Destree	Katherine G. Kuder*	Antonio Nanni	Jean François Trottier*
Ashish Dubey	David A. Lange	Nandakumar Natarajan	George J. Venta
Philip L. Dyer	John S. Lawler*	Jeffrey L. Novak*	Gary L. Vondran*
Gregor D. Fischer	Mark A. Leppert	Mark E. Patton	Robert Wojtysiak
Dean P. Forgeron*	Maria Lopez de Murphy	Max L. Porter	Robert C. Zellers
Sidney Freedman	Clifford N. MacDonald*	John H. Pye	Ronald F. Zollo
Richard J. Frost			

*Subcommittee members who prepared this report.

†Subcommittee Chair.

This document addresses the physical properties and durability of fiber-reinforced concrete (FRC). The effects of fiber reinforcement are evaluated for various physical, short-term, and long-term benefits they impart to the concrete mixture. A variety of test methods, conditions, and properties are reported. The various properties listed, in addition to the wide variety of the choices available in formulating matrix systems, allow performance-based specification of concrete materials using fibers to become a viable option. This document provides a historical basis and an overview of the current knowledge of FRC materials for tailoring new, sustainable, and durable concrete mixtures.

This document is divided into three sections. The first section discusses the physical properties of FRC in terms of electrical, magnetic, and thermal properties. Rheological properties, which affect fiber dispersion and distribution, are discussed using both empirical and quantitative

rheology. Mechanisms of creep and shrinkage and the role of various fiber types in affecting both plastic shrinkage cracking and restrained shrinkage cracking are also addressed. The durability of concrete as affected by the addition of fibers is documented under freezing and thawing, corrosion resistance, and scaling. The durability of FRC systems is also affected as different fibers respond differently to the highly alkaline cementitious microstructure. The durability of alkali-resistant glass and cellulose fibers are studied by an in-depth evaluation of long-term accelerated aging results. Degradation and embrittlement due to alkali attack and bundle effect are discussed. Recent advances for modeling and design of materials with aging characteristics are presented. Literature on the use of FRC materials under aggressive environments, extreme temperatures, and fire is presented. The final sections list a series of applications where the use of FRC has resulted in beneficial durability considerations.

ACI Committee Reports, Guides, Manuals, and Commentaries are intended for guidance in planning, designing, executing, and inspecting construction. This document is intended for the use of individuals who are competent to evaluate the significance and limitations of its content and recommendations and who will accept responsibility for the application of the material it contains. The American Concrete Institute disclaims any and all responsibility for the stated principles. The Institute shall not be liable for any loss or damage arising therefrom.

Reference to this document shall not be made in contract documents. If items found in this document are desired by the Architect/Engineer to be a part of the contract documents, they shall be restated in mandatory language for incorporation by the Architect/Engineer.

Keywords: aging; chloride permeability; corrosion; cracking; creep; diffusion; degradation; ductility; durability; electric properties; embrittlement; fiber-reinforced cement-based materials; fiber-reinforced products; fire resistance; flexural strength; freezing-and-thawing; glass; microcracking; permeability; plastic shrinkage; polypropylene; polyvinyl alcohol; reinforcing materials; rheology; shrinkage cracking; steel; sulfate attack; thermal conductivity; toughness; water permeability; wood pulp.

ACI 544.5R-10 was adopted and published March 2010.

Copyright © 2010, American Concrete Institute.

All rights reserved including rights of reproduction and use in any form or by any means, including the making of copies by any photo process, or by electronic or mechanical device, printed, written, or oral, or recording for sound or visual reproduction or for use in any knowledge or retrieval system or device, unless permission in writing is obtained from the copyright proprietors.

CONTENTS

Chapter 1—Introduction and scope, p. 544.5R-2

- 1.1—Introduction
- 1.2—Scope

Chapter 2—Notation, definitions, and acronyms, p. 544.5R-3

- 2.1—Notation
- 2.2—Definitions
- 2.3—Acronyms

Chapter 3—Physical properties of fiber-reinforced concrete (FRC), p. 544.5R-3

- 3.1—Creep
- 3.2—Shrinkage
- 3.3—Permeability and diffusion
- 3.4—Rheology
- 3.5—Electrical properties
- 3.6—Thermal conductivity

Chapter 4—Durability of FRC, p. 544.5R-13

- 4.1—Extreme temperature and fire
- 4.2—Freezing and thawing
- 4.3—Degradation and embrittlement due to alkali attack and bundle effect
- 4.4—Weathering and scaling
- 4.5—Corrosion resistance

Chapter 5—Applications and durability-based design, p. 544.5R-23

- 5.1—Case studies of applications of FRC materials and durability

Chapter 6—References, p. 544.5R-23

- 6.1—Referenced standards and reports
- 6.2—Cited references

CHAPTER 1—INTRODUCTION AND SCOPE**1.1—Introduction**

The use of fibers in concrete to improve pre- and post-cracking behavior has gained popularity. Since 1967, several different fiber types and materials have been successfully used in concrete to improve its physical properties and durability. This is supported by an extensive number of independent research results showing the ability of fibers to improve durability and physical properties of concrete. Regardless of origin, cracking, when induced by chemical, mechanical, or environmental processes, results in deteriorated and less-durable concrete. In addition, the increased permeability caused by cracking can accelerate other deterioration processes such as freezing-and-thawing damage, again resulting in less-durable concrete.

This report addresses the physical properties and durability of FRC that includes fibers in concrete. In this report, many structural systems are evaluated for various physical, short-term, and long-term benefits. These effects of using fibers have been determined using various testing methods. Many needed tests are not described by existing ASTM standards and similar standards due to the diverse nature of test methods, conditions, and properties reported. It would be a daunting task to address every project in an effort to develop correlations across the various test results. This report presents a limited collection of the published research results in relevant area. With the exception of a few characteristic responses such as creep, plastic shrinkage cracking, and long-term aging, this report does not address the mechanical properties in detail. The justification for this treatment is that topics such as mechanical properties and testing methods are addressed by subcommittees. The broader category of physical properties is in context to specific chapters.

There are several fiber types on the market intended to address various design requirements and constraints. Table 1.1

Table 1.1—A compilation of mechanical properties of commonly used fibers in concrete materials*

Type of fiber	Equivalent diameter, mm	Specific gravity, kg/m ³	Tensile strength, MPa	Young's modulus, GPa	Ultimate elongation, %
Acrylic	0.02 to 0.35	1100	200 to 400	2	1.1
Asbestos	0.0015 to 0.02	3200	600 to 1000	83 to 138	1.0 to 2.0
Cotton	0.2 to 0.6	1500	400 to 700	4.8	3.0 to 10.0
Glass	0.005 to 0.15	2500	1000 to 2600	70 to 80	1.5 to 3.5
Graphite	0.008 to 0.009	1900	1000 to 2600	230 to 415	0.5 to 1.0
Aramid	0.010	1450	3500 to 3600	65 to 133	2.1 to 4.0
Nylon	0.02 to 0.40	1100	760 to 820	4.1	16 to 20
Polyester	0.02 to 0.40	1400	720 to 860	8.3	11 to 13
Polypropylene (PP)	0.02 to 1.00	900 to 950	200 to 760	3.5 to 15	5.0 to 25.0
Polyvinyl alcohol (PVA)	0.027 to 0.66	1300	900 to 1600	23 to 40	7 to 8
Carbon (standard)	—	1400	4000	230 to 240	1.4 to 1.8
Rayon	0.02 to 0.38	1500	400 to 600	6.9	10 to 25
Basalt	0.0106	2593	990	7.6	2.56
Polyethylene	0.025 to 1.0	960	200 to 300	5.0	3.0
Sisal	0.08 to 0.3	760 to 1100	228 to 800	11 to 27	2.1 to 4.2
Coconut	0.11 to 0.53	680 to 1020	108 to 250	2.5 to 4.5	14 to 41
Jute	0.1 to 0.2	1030	250 to 350	26 to 32	1.5 to 1.9
Steel	0.15 to 1.00	7840	345 to 3000	200	4 to 10

*Data from Nawy (1996), Kuraray (2007), Saechtling (1987), Sim et al. (2005), Toledo et al. (2000), and Balaguru and Shah (1992).

Notes: 1 mm = 0.039 in.; 1 kg/m³ = 0.06 lb/ft³; 1 MPa = 145 psi; 1 GPa = 1,450,000 psi.

summarizes the majority of materials used in fiber production and the typical range of mechanical properties for each fiber type.

1.2—Scope

The report is divided into three sections:

1. The physical properties of FRC;
2. The areas where concrete durability is affected by the addition of fibers; and
3. A series of applications where FRC use resulted in beneficial durability.

The various properties addressed and the wide selection available in formulating matrix systems allow performance-based specification of concrete materials using fibers to become a viable reality. The objective of this report is to provide a historical basis about current knowledge for concrete professionals to use in tailoring new, sustainable, and durable concrete mixtures.

CHAPTER 2—NOTATION, DEFINITIONS, AND ACRONYMS

2.1—Notation

A	=	aspect ratio
C	=	capacitance, farads
C_t	=	creep coefficient at time t
C_u	=	ultimate creep coefficient
d	=	fiber diameter, in. (mm)
E_f	=	modulus of elasticity of fibers, psi (MPa)
f	=	frequency of the AC, Hz
H_R	=	relative humidity
K_s	=	thermal conductivity, BTU h ⁻¹ ft ⁻¹ °F ⁻¹ (W·m ⁻¹ °C ⁻¹)
k	=	reaction rate of the corrosion responsible for strength loss
k_o	=	frequency factor of collisions between the reactants
l	=	fiber length, in. (mm)
Q_{cr}	=	correction factor to modify for nonstandard conditions
R	=	resistance, ohms
R_u	=	universal gas constant, lb ft/(°R·lb mol) (J/(mol·K))
s	=	normalized strength
T	=	temperature, °F (K)
t	=	time, days
V_f	=	volume fraction of fibers, in. ³ (mm ³)
X	=	X-capacity reactance, ohm
Z	=	impedance, ohms
ΔG_I	=	activation energy required for the reaction to take place, ft·lb/mol (KJ/mol)
ΔT_s	=	temperature difference through the thickness of the material with known thermal conductivity, °F (K)
ΔT_u	=	temperature difference through the thickness of the material with the unknown thermal conductivity, °F (K)
τ	=	shear stress, psi (MPa)
τ_o	=	Bingham yield stress, psi (MPa)
μ_o	=	Bingham plastic viscosity, lb·s/in. ² (N·s/m ²)
$\dot{\gamma}$	=	shear rate, in./s per in. (m/s per m)

2.2—Definitions

ACI provides a comprehensive list of definitions through an online resource, “ACI Concrete Terminology,” <http://terminology.concrete.org>. Definitions provided here complement that resource.

aspect ratio, fiber—the ratio of length to diameter of a fiber in which the diameter may be an equivalent diameter (see **fiber, equivalent diameter**).

fiber, equivalent diameter—diameter of a circle having an area equal to the average cross sectional area of a fiber.

tex—the mass in grams of 3280 ft (1 km) of strand or roving.

2.3—Acronyms

AASHTO—American Association of State Highway Transportation Officials

AC—alternating current

AC-IS—alternating current-impedance spectroscopy

AR—alkali-resistant

ARS—average residual strength

ASM International—The Materials Information Society

ASTM International—American Society for Testing and Materials

CAC—calcium aluminate cement

DC—direct current

DW—drawing-wire

FRC—fiber-reinforced concrete

FRCB—fiber-reinforced cement board

GFRC—glass fiber-reinforced concrete

HAC—high-alumina cement

HSC—high-strength concrete

IPC—inorganic phosphate cement

IS—impedance spectroscopy

NSC—normal-strength concrete

OPC—ordinary portland cement

PP—polypropylene

PVA—polyvinyl alcohol

SAC—sulfo-aluminate cement

SFRC—steel fiber-reinforced concrete

CHAPTER 3—PHYSICAL PROPERTIES OF FIBER-REINFORCED CONCRETE (FRC)

3.1—Creep

Creep is defined as a phenomenon in which strain in a solid increases with time while the stress producing the strain is kept constant. In more practical terms, creep is the increased strain or deformation of a structural element under a constant load. Depending on the construction material, structural design, and service conditions, creep can result in significant displacements in a structure. Severe creep strains can result in serviceability problems, stress redistribution, prestress loss, and even failure of structural elements. For some other structural elements such as bridge decks, however, severe creep strains can result in serviceability benefits.

3.1.1 Creep behavior of concrete—Concrete is known to deform considerably under constant loading and normal service conditions. Compressive creep strain in conventional concrete can be 1.30 to 4.15 times the initial elastic strain under standard conditions (ACI 209R; Troxell et al. 1958).

For certain non-standard conditions, such as low ambient relative humidity or high ambient temperature, creep strain can be even greater. Over time, these large creep strains result in shortened compression members and increased deflections in bending members.

The creep coefficient C_t is defined as the ratio of creep strain to initial elastic strain and is dependent upon the time t after application of stress. The method suggested in ACI 209R is most commonly used for predicting the creep behavior of concrete, using the following expression that is applicable for normal- to low-density concrete:

$$C_t = \frac{t^{0.6}}{10 + t^{0.6}} C_u Q_{cr} \quad (3-1)$$

where C_t is the creep coefficient at time t (days) after application of stress; C_u is the ultimate creep coefficient; and Q_{cr} is a correction factor to modify for nonstandard conditions. ACI Committee 209 intended for this expression to be used only if the sustained compressive stress is less than or equal to 50% of the concrete strength.

3.1.2 Creep behavior of fibers—Polymeric fibers are considered as viscoelastic materials and are more susceptible to creep than metallic and glass fibers. They tend to respond to short-time stresses in an elastic fashion. If a relatively high stress level is maintained for considerable time, however, polymeric materials will behave viscously and will creep, even exhibiting creep rupture (ASM International 1988). The strain to failure is usually high enough for stress redistribution and relaxation to take place, accommodating the deformation. Steel fibers do not exhibit creep behavior under normal service conditions at temperatures below approximately 700°F (370°C) (ASM International 1990).

3.1.3 Creep behavior of FRC—Given the low fiber dosages typically used in concrete (0.1 to 1% vol.), the presence of fibers (steel, synthetic, glass, cellulose) has a minimal, if any, impact on the creep behavior of concrete in compression. The flexural creep performance of conventionally reinforced concrete beams incorporating steel fiber-reinforced concrete (SFRC) showed smaller long-term deflections than the reinforced concrete beams without fibers (Tan et al. 1994).

The addition of fibers primarily benefits the post-crack behavior of concrete. The post-crack creep of FRC studied by Balaguru and Kurtz (2000) indicated that creep failure occurred in cracked micro-synthetic FRC for sustained stress levels. The definitions of macro- and micro-fibers can be found in ACI 544.3R. Micro-synthetic FRC could only sustain a small percentage of the post-crack stress. Creep of the fiber/matrix interface bond was an important aspect because most FRC mixtures are designed to fail in pullout mode rather than fiber-fracture mode.

The addition of macro- and micro-fibers (ACI 544.3R) primarily benefits the post-crack behavior of concrete. The post-crack creep of FRC studied by Balaguru and Kurtz (2000) indicated that creep failure occurred in cracked micro-polymeric FRC for sustained stress levels. Micro-polymeric FRC could only sustain a small percentage of the

post-crack stress. Creep of the fiber/matrix interface bond was an important aspect because most FRC mixtures are designed to fail in pullout mode rather than fiber-fracture mode.

The magnitude of load applied to a specific specimen during creep testing was based on the results of average residual strength (ARS) tests determined using ASTM C1399. Prior to creep testing, the beams were cracked by subjecting 4 x 4 x 14 in. (100 x 100 x 350 mm) beams to a deflection of 0.01 in. (0.2 mm). Specimens of the synthetic FRC mixture were creep tested at loads nominally equivalent to 20, 40, and 60% of the ARS value while the SFRC mixture was tested at loads nominally equivalent to 20, 40, 60, and 80% of the ARS value. The study concluded that, at similar loading levels, cracked synthetic FRC can be expected to experience creep coefficients twice that of SFRC.

Bernard (2004a) studied the creep of cracked FRC specimens and round panels based on ASTM C1550. High-modulus synthetic macrofibers, crimped low-modulus synthetic macro-fiber, and flat-end steel fiber were investigated for long-term creep behavior in cracked concrete specimens. Results indicated that the high-modulus synthetic macrofiber had creep behavior similar to the steel fiber, whereas the low-modulus synthetic macrofiber experienced much higher creep.

3.2—Shrinkage

Fibers can be added to concrete to reduce cracking potential due to shrinkage. Plastic shrinkage occurs during the early-age period when the strength of the paste is quite low, and drying shrinkage occurs due to volume change after the concrete hardens. If the shrinkage deformation is sufficiently restrained, the tensile stresses generated may be sufficiently high to cause cracking. The addition of synthetic or cellulose microfibers has been shown to increase the strength and strain capacity sufficiently during the very early ages (up to 12 hours) so that the potential for cracking under the tensile stresses generated by the shrinkage is minimized. Adding steel and macro-synthetic fibers has been shown to provide strength- and strain-carrying capacity after the concrete has hardened to the extent that the FRC resists and controls drying-shrinkage cracking. Understanding these principles is essential when designing durable structures.

Over the last century, several test methods have been used to evaluate the plastic and restrained shrinkage cracking behavior of mortar and concrete. While a wide range of tests are available, two tests have been standardized by ASTM to evaluate early-age cracking. The first test method, ASTM C1579, focuses on assessing the plastic shrinkage cracking behavior of concrete. This method uses a stress riser to simultaneously simulate the effects of evaporation, autogenous shrinkage, and settlement (Berke and Dalliare 1994). The stress riser, which focuses on a crack in a small region in the center of the sample, is intended to simulate conditions that occur above a reinforcing bar in practice (Qi and Weiss 2003; Qi et al. 2003; Banthia and Gupta 2006). The second test method, ASTM C1581, uses the restrained ring geometry to describe the restrained drying shrinkage cracking behavior of hardened concrete. Although the standardized testing procedure is relatively new, this testing approach has

been in use for cement pastes, mortars, and concretes for nearly a century. A review of developments in ring testing has been published (Radlinska et al. 2006) and the American Association of State Highway Transportation Officials (AASHTO) PP34 also recommends a provisional standard for performing a ring test.

3.2.1 Plastic shrinkage cracking—Numerous researchers have studied the effects of fibers on plastic shrinkage cracking behavior. A general observation is that a finer fiber is more effective in reducing the width of plastic shrinkage cracks than a coarse fiber (Qi and Weiss 2003; Banthia and Gupta 2006). Most fine-diameter microfibers with a high specific fiber surface area are particularly effective in reducing plastic shrinkage cracking.

Naaman et al. (2005) evaluated the effect of several fibers on the plastic shrinkage cracking characteristics of concrete including polypropylene (PP), PVA, Spectra, carbon, and steel, covering a wide range of properties. Prismatic concrete specimens freshly cast on top of a grooved, hard concrete substrate were subjected to adverse environmental conditions, namely, elevated temperature, low relative humidity, high volume, and airflow velocity. Testing parameters covered a range of fiber properties, including diameter, length, cross section, form, bond strength, and elastic modulus. Experimental results indicated that volume fraction and diameter of fiber reinforcement are the two most influential parameters in controlling plastic shrinkage cracking of concrete. For a given volume fraction of fibers, changing the fiber length or aspect ratio did not have a noticeable effect on plastic shrinkage cracking. Decreasing the fiber diameter or equivalently increasing the number of fibers crossing a unit area, however, did significantly improve the control of plastic shrinkage cracking. At a volume fraction of 0.2%, most fine-diameter polymeric fibers tested provided a reasonable control of plastic shrinkage cracking, reducing it to approximately 10% of control.

Najm and Balaguru (2002) studied the effect of polymeric fibers on the reduction of crack width caused by plastic and drying shrinkage. The variables included matrix composition, fiber geometry and aspect ratio, and fiber volume fraction, which ranged from 7.5 to 45 lb/yd³ (4.5 to 27 kg/m³). Fibers increased the strain capacity and reduced the crack width compared to control samples without reinforcement. An approximate fiber content of 15 lb/yd³ (9 kg/m³) resulted in a 60% reduction in crack width. In addition, polymeric macrofibers provided the same reduction in width of cracks as steel fibers at half the fiber volume fraction. Note that crack reductions include both plastic and drying shrinkage.

The shape of fiber effects were also studied by Ma et al. (2002) who evaluated different cross sections of PP microfibers. Test results showed that PP microfibers with circular cross section made by a drawing-wire (DW) technique had a more pronounced effect on the resistance to plastic shrinkage cracking than PP microfibers with rectangular cross section made by a fibrillated film technique. Polypropylene microfibers with a Y-shape cross section were slightly more effective in reducing plastic shrinkage cracking than the DW-PP fibers.

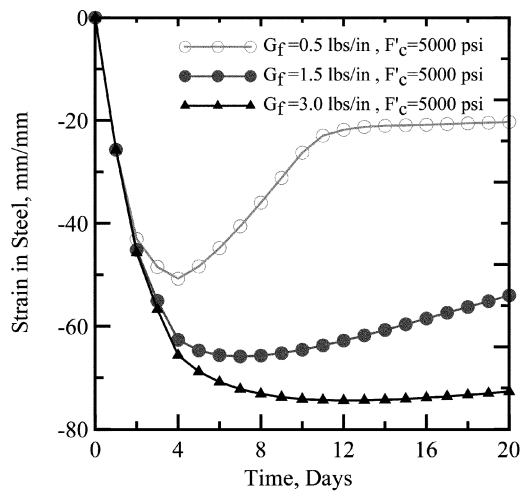
Banthia et al. (1996) and Banthia and Yan (2000) studied the plastic shrinkage cracking in polyolefin FRC using a substrate restraint type shrinkage test. Polyolefin fibers were generally effective in reducing the amount and size of shrinkage cracking, and their dimensions decisively influenced the results. Although crack widths were reduced from 0.005 in. (1 mm) in plain concrete to less than 0.002 in. (0.40 mm) with 0.7% by volume of the 2 in. (50 mm) long fibers, they were completely eliminated as the fiber length was reduced for similar levels of aspect ratio and volume fraction.

Qi et al. (2003) and Qi and Tianyou (2003) used image analysis to systematically characterize the size of the plastic shrinkage cracks that developed. They found it crucial to use a large set of measurements to obtain statistically reproducible results because of the large variation typical in crack width measurements. In addition to a reduction in the width of the plastic shrinkage cracks, fibrillated fibers were effective in reducing the rate of corrosion (Qi et al. 2006).

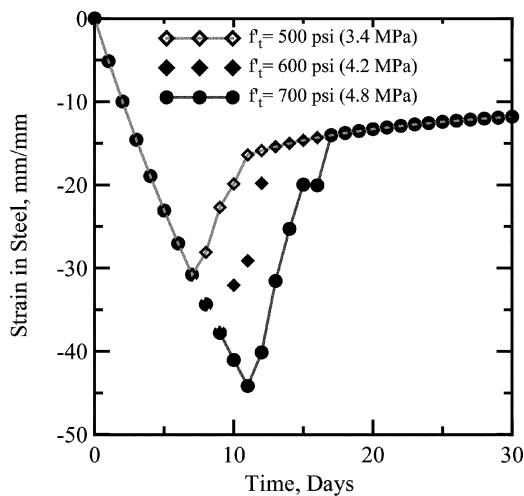
Wongtanakitcharoen and Naaman (2007) evaluated the plastic shrinkage cracking characteristics of concrete containing PP, polyvinyl alcohol (PVA), high-density polyethylene (HDPE), carbon, and metallic fibers during the first 24 hours after mixing. Testing parameters cover several fiber properties, including diameter, length, cross section, form, bond strength, and elastic modulus that were investigated under high temperature, low relative humidity, and high airflow volume and velocity. Results indicate that volume fraction and diameter of fiber reinforcement are the two most influential parameters in controlling plastic shrinkage cracking of concrete. For a given volume fraction of fibers, changing the fiber length or aspect ratio did not have a noticeable effect on plastic shrinkage cracking, whereas decreasing the fiber diameter significantly improved the plastic shrinkage cracking resistance. At a volume fraction of 0.2%, most fine-diameter fibers tested provided a reasonable control of plastic shrinkage cracking, reducing it to approximately 10% of control. Plain concrete mixtures shrink less at very early ages, presumably due to the bleed water that remains on the surface of the specimen for a longer time. Much of the shrinkage occurs before the mortar sets (as identified by the change in the slope of the shrinkage curve [Sant et al. 2006]).

3.2.2 Restrained shrinkage cracking—Bissonnette et al. (2000) conducted uniaxial restrained shrinkage tests and tensile tests on large-scale SFRC specimens with fiber contents ranging from 0 to 160 lb/yd³ (0 to 100 kg/m³). Multiple parallel microcracks altered the overall response of the SFRC beams in the hardened state.

Several recent studies have evaluated the influence of ring geometry and drying direction on the behavior of the restrained shrinkage test using the steel ring specimen (Swamy and Stavarides 1979; Hossain et al. 2003; Hossain and Weiss 2004). These studies demonstrated how the steel ring could be used to directly measure the residual stress that develops in the concrete as well as the stress relaxation that occurs. Mane et al. (2002) developed an experimental and analytical simulation algorithm to study the restrained shrinkage cracking in plain and fiber-reinforced concrete.



(a)

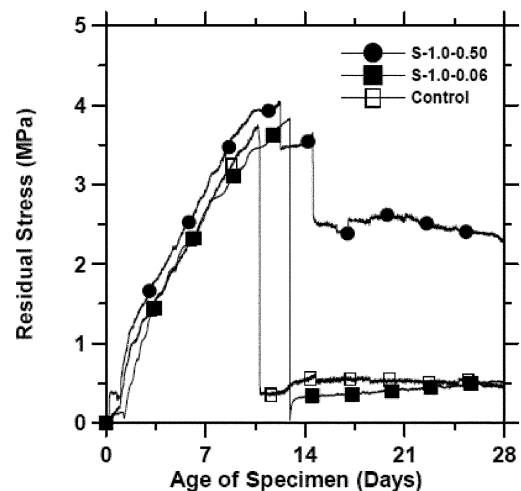


(b)

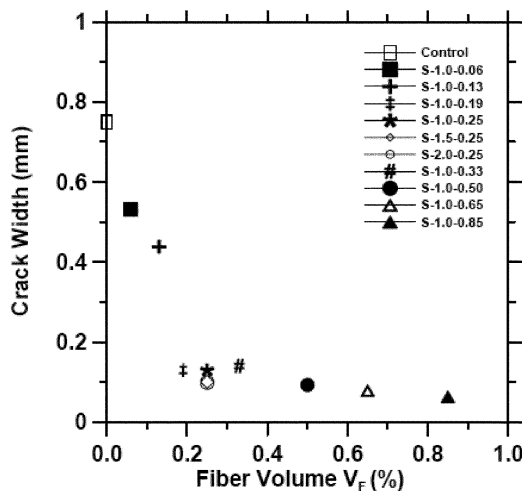
Fig. 3.1—Theoretical curve of restrained shrinkage test illustrating the effect of fracture energy and tensile strength of concrete (Mane et al. 2002): (a) effect of fracture energy of the FRC material representing an increase in fiber content on the stress relaxation in steel; and (b) effect of tensile strength of concrete with a proportional increase in fracture energy.

The effect of the geometry of the specimens, the humidity and shrinkage conditions, the restraint offered by the stiffness of the steel ring, and the concrete properties such as stiffness, shrinkage, and creep were studied using an analytical approach. The model is based on the stress analysis of a restrained concrete section and includes shrinkage, creep, aging, and microcracking. Using the theoretical models, it is possible to calibrate and interpret the experimental test results.

Figure 3.1(a) represents the theoretical curve of strain in the steel as a parametric study of the effect of fibers. The compressive stress builds up gradually in the steel, and as the concrete cracks from a tensile failure mode, there is a gradual relaxation and recovery of strain in steel. The strain in the steel does not decay as quickly as cracking takes place in the specimen, if the fracture energy is sufficiently high, which indicates the load transfer can take place. Figure 3.1(b)



(a)



(b)

Fig. 3.2—Influence of steel fibers volume on residual stress development and the influence of steel fiber volume on the crack width (Shah and Weiss 2006). (Notation: S-X-Y, X = fiber length, in.; Y = fiber volume, %.)

shows the effect of concrete strength on the cracking response. Only the first cracking point is affected as the tensile strength is increased. The first crack formation in the theoretical model is after 8 days, which is similar to the experimental results. Beyond the cracking of concrete, its creep properties in the post-peak region contribute to an increase in strain, causing further reduction of steel strain. Shah and Weiss (2006) demonstrated that, prior to cracking, the stresses that develop in plain concrete and in FRC are very similar (Fig. 3.2). They also developed an analytical procedure to describe how the strain that develops in the steel ring can be used to estimate the stress transferred across the crack and the size of the crack that develops in the ring; however, they also indicated that the small geometry of the ring may result in smaller crack widths and higher stress transfer than what may be expected in practice.

Voight et al. (2004) compared the performance of different fiber types, fiber blends, and welded-wire reinforcement in their ability to prevent and control drying-shrinkage

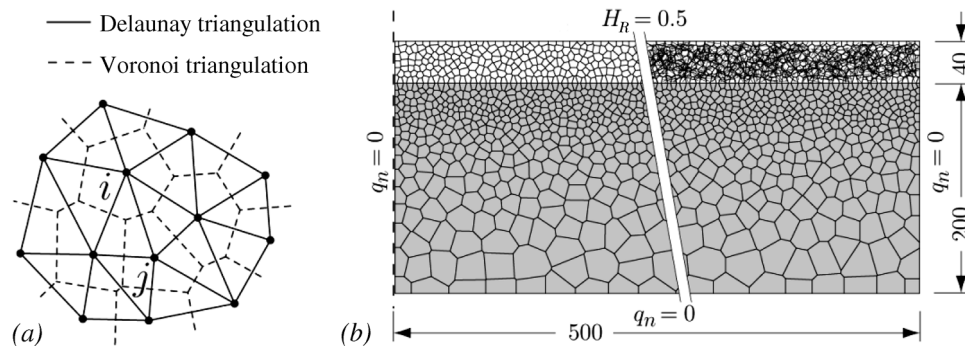


Fig. 3.3—(a) Element ij within irregular lattice; and (b) computational grid for simulating drying of an overlay system (fiber composite overlay shown on right side; dimensions are in mm) (Bolander and Berton 2004) (1 mm = 0.039 in.).

cracking. This program used the AASHTO PP34 ring shrinkage test to force cracks to occur in samples due to drying shrinkage. Several conclusions were made from the test. First, they concluded that fiber count is not a good indicator of controlling drying-shrinkage cracks. Approximately the same level of crack control is achieved by the same dosage of profiled 0.8 in. (20 mm), flat-end 1.2 in. (30 mm), and hooked-end 2 in. (50 mm) fibers, regardless of a significant difference in the fiber count. Second, a reasonable indicator of maximum crack width can be correlated to the value of the fiber volume V_f times the aspect ratio A . Therefore, fiber-reinforced concretes that have the same value for $V_f A$ provide a similar level of crack control. When volume or dosage rate is held constant, fibers with similar aspect ratios provide the same level of crack control.

Various models have been developed for predicting transverse cracking of concrete ring specimens due to drying shrinkage (Shah et al. 1998). These models have been developed based on nonlinear fracture mechanics. Using the measured material fracture parameters, the fracture resistance curve (R -curve) of the ring specimen is determined. Another model has been developed for a compatibility condition that equates the difference between measured free shrinkage and estimated creep with the maximum allowable tensile strain (Mane et al. 2002). Based on this condition, age at transverse cracking of the specimen subjected to restrained drying shrinkage can be predicted.

A model was proposed for predicting the shrinkage of SFRC from the composition of concrete mixture, strength, age when drying begins, conditions of environment, size and shape of structures, fiber volume ratio, and aspect ratio of the fiber (Young and Chern 1991). The model is based on the well-developed Bažant-Panula (BP) model for the shrinkage of plain concrete (Bažant et al. 1991; Bažant and Panula 1978). All important features of the BP prediction model, such as the diffusion-type size dependence of humidity effects and the square-root hyperbolic law for shrinkage, are adopted for SFRC.

Zhang and Li (2001) presented a model to predict the drying shrinkage performance of a fiber-reinforced cementitious composite. A free shrinkage expression is presented to show the influence of the matrix and fiber properties and fiber

orientation characteristics. Model results indicate that shrinkage of a fiber-reinforced cement-based composite is significantly influenced by the elastic modulus of the fiber and the matrix, as well as fiber length and diameter.

Bolander (2004) and Bolander and Berton (2004) have developed irregular lattice models of FRC in which the primary material phases—for example, fiber, matrix, and interfacial zone—are represented as separate entities (Fig. 3.3). The modeling of moisture diffusion, convective boundary conditions at exposed surfaces, and coupling of the stress and diffusion analyses are based on the works of Bažant and Najjar (1971) and Martinola and Wittmann (1995). Short fibers are explicitly modeled within the three-dimensional domain, directly accounting for length and orientation efficiency of each fiber and wall effects that can bias fiber orientations near the domain boundaries. Fiber distributions can be numerically generated, as has been done in cited works, or obtained from actual tests such as computed tomography. One objective is to simulate the effects of directional bias and non-uniformity of fiber distributions.

The lattice model has been used to study drying-shrinkage cracking in a fresh cement composite overlay on a mature concrete substrate and the role of fibers in restraining such cracking. Figure 3.3 shows a lattice discretization of the composite system. The lattice topology is based on the Delaunay triangulation of an irregular set of nodal points, whereas the dual Voronoi diagram serves to define the element properties. The overlay, substrate, and an interfacial layer are defined by their elasticity, hygral, and fracture properties. The upper face of the lattice model is exposed, via a convective boundary condition, to an environment with relative humidity $H_R = 0.5$, whereas the overlay and a portion of the substrate are assigned relative humidity $H_R = 1.0$. With exposure to the drying environment, the moisture diffusion analysis produces humidity gradients that lead to stress development in the overlay system. Without fiber reinforcement, fracture zones develop rather uniformly along the top of the overlay prior to 20 days of exposure to drying. With shrinkage due to additional drying, localization occurs as characterized by several of the cracks continuing to open while neighboring cracks unload. A maximum crack opening of 0.014 in. (0.29 mm) occurs after 110 days of

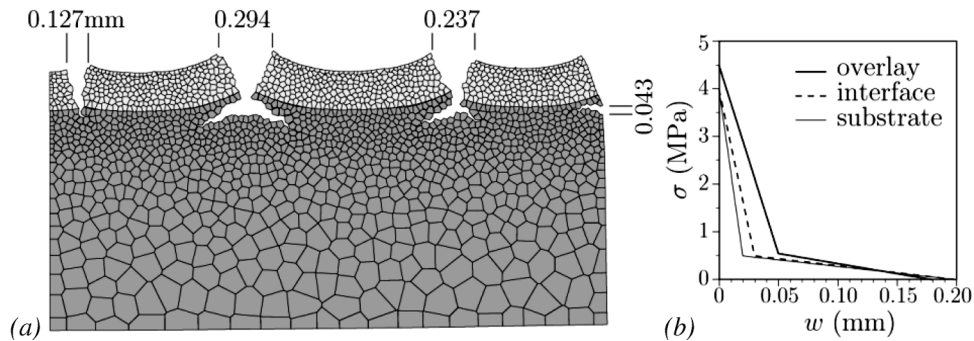


Fig. 3.4—Unreinforced overlay: (a) damage pattern after 110 days of exposure to drying environment; and (b) stress versus crack opening relations for system components (Bolander and Berton 2004). (Note: 1 mm = 0.039 in.; 1 MPa = 145 psi.)

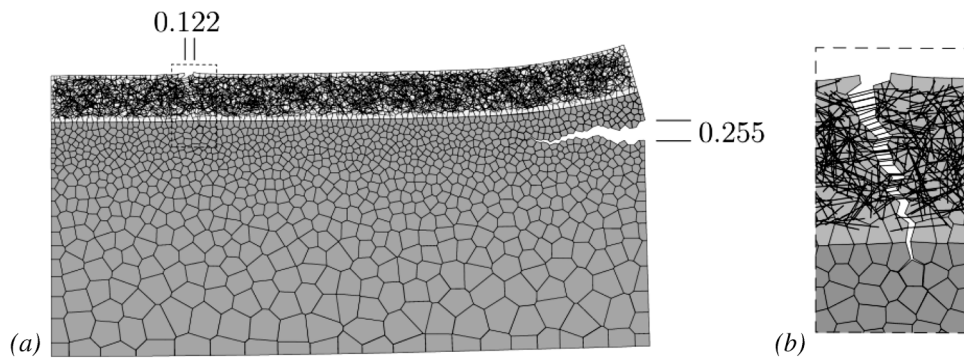


Fig. 3.5—Fiber-reinforced overlay: (a) damage pattern after 110 days of exposure to drying environment; and (b) fibers bridging a crack in the overlay (dimensions in mm) (Bolander and Berton 2004). (Note: 1 mm = 0.039 in.)

drying (Fig. 3.4(a)). The pattern of cracks in the overlay, as well as the tendency for vertical overlay cracks to turn and run laterally, are in good general agreement with the results presented by Martinola and Wittmann (1995). When PVA fibers (diameter = 0.005 in. [0.12 mm], length = 1.5 in. [39 mm], $E_f = 6 \times 10^6$ psi [42.8 GPa], $V_f = 2\%$) are introduced into the overlay material, diffuse microcracking still occurs along the top of the overlay, but only one smaller crack runs through the thickness of the overlay. The fibers restrict the opening of this crack to 0.005 in. (0.12 mm) after 110 days of drying, and the undesirable lateral branching of cracks is also arrested (Fig. 3.5). The fibers restrict the opening of this crack to 0.0005 in. (0.12 mm) in the overlay after 110 days of drying and the undesirable lateral branching of cracks is also arrested (Fig. 3.5). Due to restraining the width of cracks by fibers in the overlay, relief is achieved by horizontal cracks developing in the substrate, starting from the edge of the overlay/substrate system.

3.3—Permeability and diffusion

Concrete is susceptible to degradation through corrosion, alkali-silica reaction, sulfate attack, freezing-and-thawing damage, and other mechanisms that result from the ingress of water. Concrete durability is, therefore, intimately related to the rate at which water is able to penetrate it (water permeability). Fiber-reinforced concrete has been used in applications where water-tightness is desired, such as tunnel linings and

liquid storage tanks (Bentur and Mindess 1990; Mindess et al. 2003). The permeability of dense concrete, such as that with a water-to-cement ratio less than approximately 0.45, is nearly negligible in an uncracked condition. Permeability, however, is vastly increased by the introduction of cracks and increases with crack width (Ludirdja et al. 1989; Wang et al. 1997). Fiber reinforcement influences the way cracks develop in concrete and may impart improved crack growth resistance, increased surface roughness of individual cracks, and a greater likelihood for crack branching and multiple crack development. Due to this, fiber reinforcement may be used to significantly reduce the permeability of cracked concrete.

A number of studies have been conducted to investigate the relationship between FRC and water permeability. Tsukamoto and Wörner (1991) studied the permeability of cracked FRC using uniaxial tension tests of notched-rectangular prisms. A reduction in flow rate through the reinforced specimen was observed versus an unreinforced specimen deformed by the same amount. Aldea et al. (2000) evaluated the effect of fiber length and crack width (0 to 0.012 in. [0 to 300 μ m]) on water permeability and resistance to penetration of chloride ions of PVA fiber-reinforced mortars at an unloaded state, in which a crack had been induced using a tensile splitting configuration. It was observed that when fibers initiated crack branching, a lower water permeability resulted. Water permeability was significantly more sensitive

than resistance to chloride ion penetration within the crack range studied. Rapoport et al. (2002) and Aldea et al. (2001) studied the effect of steel fiber volumes (0, 0.5, and 1%) and crack width (0 to 0.012 in. [0 to 300 μm]) on low-pressure water permeability of steel fiber-reinforced normal-strength concrete (NSC) at an unloaded (relaxed) and loaded state, respectively, in which cracks were induced by a feedback-controlled splitting tension test. In conclusion, the steel fibers decreased the permeability of specimens for cracks larger than 0.004 in. (100 μm), whereas below 0.004 in. (100 μm), they do not seem to affect the permeability of concrete. Lawler et al. (2002) evaluated the relationship between multiple cracking, fiber reinforcement, and permeability by measuring the water permeability of fiber-reinforced mortars during uniaxial tensile tests on unnotched specimens. This method of testing permitted distributed multiple cracks to develop, and as a result, this study found that a significant reduction in water flow rate at a given displacement is possible with fiber reinforcement, depending on the fiber type and volume. The flow rate versus uniaxial tensile displacement for mortar containing various levels of reinforcement is shown in Fig. 3.6.

To directly investigate the effects fibers have on the durability of concrete structures, Sanjuán et al. (1997) included PP fibers in the cover over conventional steel reinforcement. Mortar was cast around steel bars in specimens that were then exposed to restrained shrinkage conditions immediately after casting. After curing, the specimens were ponded with a chloride ion-rich solution while the rate of corrosion in the steel was monitored. Fiber-reinforced matrixes cracked less and demonstrated lower corrosion rates showing the direct impact of fibers on permeability-related deterioration mechanisms.

Concrete materials that contain cracks of approximately 0.004 in. (100 μm) in width show a substantial increase in water permeability both for plain concrete (Wang et al. 1997) and FRC (Aldea et al. 2001; Lawler et al. 2002). This suggests a threshold level for use as a design criterion below which crack widths should be maintained to maximize the durability of concrete structures. While further work is required to confirm a relationship between crack width and concrete durability, one potential means to achieve such a criterion is with fibers. Further discussion about this can be found in Section 3.5 of ACI 224.2R regarding the relationship between crack width and serviceability.

Gas permeability is another method that is commonly used to evaluate durability characteristics of concrete. Picandet et al. (2001) examined the effect of axial compressive loading on the permeability of three different types of concrete: ordinary, high-strength, and steel fiber-reinforced concrete. Monotonic and cyclic loads were applied on 8 x 4 in. (200 x 100 mm) diameter specimens using stress levels between 60% and 90% of the ultimate strength. At the end of the loading phase, a disc was extracted from the middle part of the cylinders, and four different gas permeability tests were conducted during the drying procedure. A relationship between mechanical damage indicators and the increase in permeability was proposed.

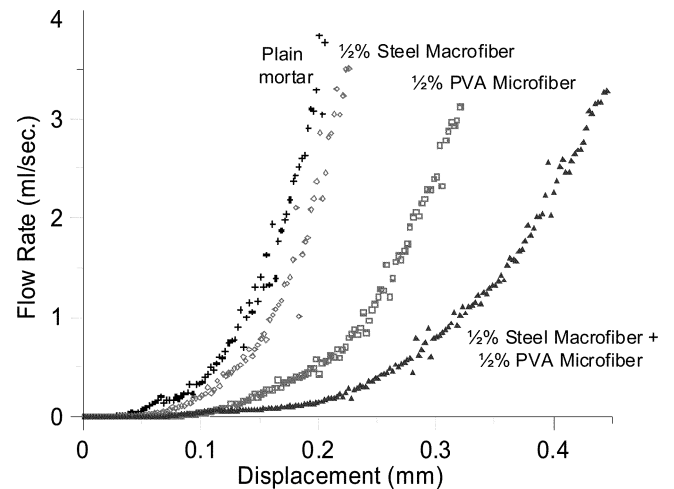


Fig. 3.6—Flow rate versus uniaxial tensile displacement for mortar specimens containing various levels of reinforcement (Lawler et al. 2002).

3.4—Rheology

The characteristics of FRC in a fresh state can be described using rheological parameters that characterize flow, or deformation, under stress. These parameters enable workability, flow, pumping ability, placement, compaction, and finishing characteristics to be quantitatively monitored and used during the construction phase.

A variety of test methods exist to describe the rheological properties. Tattersall (1991) classified three test categories: qualitative, quantitative-empirical, and quantitative-fundamental. Qualitative tests are subjective. Quantitative-empirical methods give limited information about flow behavior under certain conditions and include the slump test, vebe flow time, and inverted cone test. Quantitative-fundamental tests measure true material flow properties. These properties are typically evaluated using rheometers, which measure a material's response to shear. While measuring the fundamental flow properties of FRC is preferred, it is difficult with conventional rheometers, which are only suited for small sample sizes and highly flowable materials.

3.4.1 Empirical rheology—Researchers have studied the influence of fibers on the rheology of FRC for over 25 years. A number of parameters affect flow behavior, including the physical characteristics, fiber content, matrix properties, aggregate content, and the processing methods. Two of the most prominent factors affecting flow are the aspect ratio (fiber length/diameter) and the volume fraction of fibers. The combined effect of these two parameters is defined as “reinforcement index,” or “fiber factor” as $(l/d) \times V_f$, where l = fiber length, d = fiber diameter, and V_f = volume fraction of fibers (Hughes and Fattuhi 1976).

Early work relied on quantitative empirical tests to evaluate the flow behavior of SFRC. Researchers found that the key factors affecting rheology were the fiber volume, aspect ratio, type, and geometry. Hughes and Fattuhi (1976) showed that workability decreases proportionately with $(l/d)^{1/2} \times V_f$. Swamy and Mangat (1974), Mangat and Swamy (1974), and Bayasi and Soroushian (1992) showed

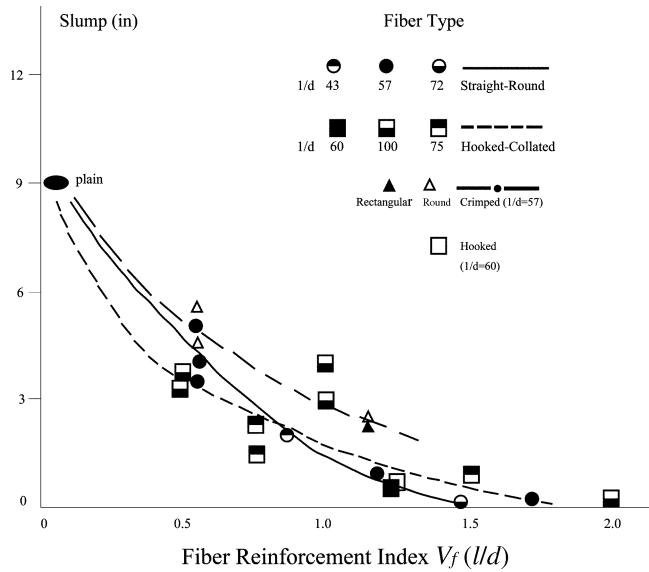


Fig. 3.7—Effect of fiber reinforcement index and type on slump (Bayasi and Soroushian 1992).

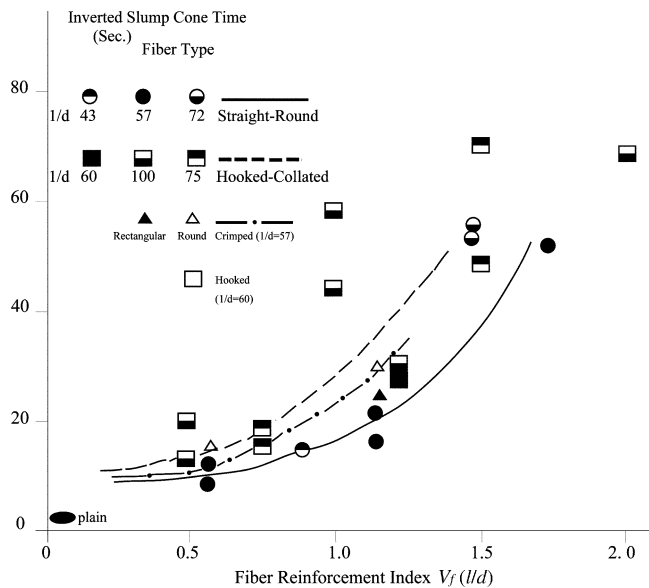


Fig. 3.8—Effect of fiber reinforcement index and type on inverted slump cone time (Bayasi and Soroushian 1992).

that the fresh-state properties worsen as the fiber reinforcement index increases, and that the rate of change is directly related to the fiber type. Varying steel fiber geometries were evaluated, including straight-round, hooked-end, duoform, and crimped (deformed continuously along the length) fibers. Generally, crimped fibers were shown to have slightly higher workability than the other geometries. Figures 3.7 and 3.8 present results from Bayasi and Soroushian (1992) that show the effects of fiber reinforcement index on the slump and inverted cone time, respectively.

To improve the fresh state properties of SFRC, collated fibers were developed. These fibers have deformed ends that are adhered together using water-reactive glue. Thus, as the fibers are first added to the mixture they have a lower aspect

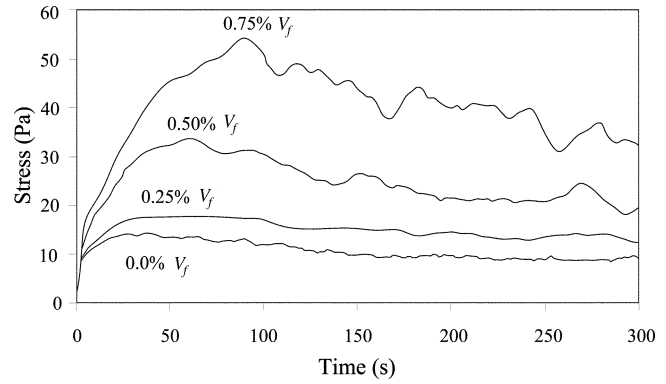


Fig. 3.9—Effect of cellulose fiber content on the yield stress of neat paste ($w/c = 0.50$) measured with a commercial rheometer using the vane configuration (Rapaport and Shah 2005).

ratio, facilitating better mixing. Ramakrishnan et al. (1980) and colleagues found that the dispersion of hooked-end fibers improved with the use of the collated fibers. Giaccio et al. (1986) studied the effect of mixing time on the separation of individual fibers from bundles, which is needed to get the full mechanical advantage of the fibers. Research indicated that shorter mixing times were better for workability, but were not sufficient for separating the fibers.

3.4.2 Quantitative rheology—Recently, researchers have attempted to obtain flow properties of FRC by using rheometers. Two categories of rheometers are considered: commercially available and custom designed. Commercially available rheometers were originally developed for polymer systems and allow for different geometries such as the parallel plate, coaxial cylinder, and vane configurations used as interchangeable fixtures of a single machine. Small sample sizes and a low torque capacity, however, limit the testing to relatively fluid cement paste and mortar systems, typically without fiber reinforcement. In response to these limitations, a number of research grade rheometers have been developed for highly fluid concrete materials. Custom designed rheometers include mixer-type setups (Beaupre 1994; Struble et al. 2001; Tattersall and Bloomer 1979), coaxial cylinder configurations (Coussot 1993; Wallevik and Gjrv 1990), and parallel plate geometries (Hu et al. 1996), as well as the rheometer developed at the University of Illinois at Urbana-Champaign (Struble et al. 2001).

A number of different models exist to describe the rheological characteristics of cementitious systems. The most commonly used model is the Bingham model, which is given by

$$\tau = \tau_o + \mu_o \dot{\gamma} \quad (3-2)$$

where τ_o is the Bingham yield stress describing the stress needed to initiate flow; μ_o is the Bingham plastic viscosity, which is the resistance of the material to flow; and τ and $\dot{\gamma}$ are the shear stress and shear rate, respectively. Malek and Roy (1991) reviewed other models, including the Herschel-Bulkley, Vom Berg, Casson, Ellis, Eyring, Robertson-Stiff,

Williamson, Sisko, and Atzeni. Flow curves obtained with rheometers are used to fit the data to these models.

Rapoport and Shah (2005) used a commercial scale rheometer to describe the rheology of cellulose fiber-reinforced cement paste and mortar. The peak yield stress of the mixtures was determined using the vane geometry. Yield stress curves are shown in Fig. 3.9 and indicate that the yield stress increases as the amount of cellulose fibers increases. Because a commercial rheometer was used, the viscosity of the fiber-reinforced pastes and mortars could not be obtained for these stiff mixtures. The authors, therefore, evaluated the viscosity of the matrix only and used this information to describe the flow behavior of the entire system.

Bui et al. (2003) evaluated the effects of steel and PP fibers on the flow behavior of highly fluid mortar using a concentric cylinder rheometer (Wallevik and Gjørv 1990). The Bingham parameters were used to describe flow. They found that the rheology of the mortar was influenced by fiber content, the ratio between the fiber volume fraction and maximum packing density of fibers, the radius and length of the fibers, and the properties of the matrix.

A custom-designed and built parallel plate rheometer was developed by Kuder and coworkers to evaluate the rheology of stiff fiber-reinforced cement pastes and mortars (Kuder et al. 2004). The effect of steel fiber volume on the rheological parameters was studied. Bingham yield stress and viscosity decreased with increased fiber content until a critical volume fraction was reached. This trend was explained by a coupling effect between the structural breakdown of the cement paste, which occurs at low fiber volumes, and the mechanical interlocking of the fibers, which occurs at higher volume fractions. These results demonstrate the potential differences in rheological trends when stiffer cementitious systems are investigated.

3.4.3 Relating rheology, fiber dispersion, and mechanical performance—Fiber dispersion is known to affect the mechanical performance of FRC. Because fiber dispersion is influenced by fresh-state properties, researchers have begun to link rheology, fiber dispersion, and mechanical performance. Ferrara (2003) and Özyurt et al. (2006a) used viscosity-modifying admixtures to improve fiber distribution in steel SFRC. The improvement in fiber distribution also led to an enhancement of mechanical properties.

While the effects of fibers on the rheology of the FRC have been studied for many years, our understanding of these systems is limited. The development of new rheometers suitable for testing these systems allows for fundamental flow properties to be identified. With an improved understanding of how fibers affect rheology, FRC can be designed so they are easy to work with during the fresh state to achieve the desired hardened-state properties.

3.5—Electrical properties

Many research studies have concentrated on using electrical methods as a means of characterizing concrete and developing potential applications for new materials, nondestructive testing, or diagnostic equipment (McCarter 1996). Various test results support the concept that the electrical conductivity of concrete is essentially electrolytic by ion transport through

the interconnected pore network. The electrical resistance of concrete ranges by several orders of magnitude between a moist-cured condition and oven-dried (Hammond and Robson 1955). Concrete is thought to behave as a parallel circuit of a capacitor and resistor. Its impedance to an alternating current (AC) is

$$\frac{1}{Z^2} = \frac{1}{X^2} + \frac{1}{R^2} \quad (3-3)$$

where Z = impedance, ohms; R = resistance, ohms; $X = 1/fC$ = capacitive reactance, ohms; f = frequency of the AC, Hz; and C = capacitance, farads.

For an AC, the capacitive reactance is always much greater than the resistance because the capacitance is small, which implies that the overall impedance using AC power is nearly equal to the direct current (DC) resistance. Following the introduction of a technique known as alternating current-impedance spectroscopy (AC-IS), researchers have concentrated on the use of the equivalent circuit modeling for the microstructural characterization of concrete at various stages of hydration (Christensen et al. 1994; McCarter and Brosseau 1990; Gu et al. 1992a,b).

Carbon or steel fibers can be added to a cement matrix at a high volume fraction of 0.5 to 3% (in further examples cited) to increase the conductivity of the composite. The mechanical status of the cement composite can affect the electrical properties (DC resistance and AC impedance) of the composite. Measurements of these electrical properties can be used as an indirect, nondestructive test for cement composites, making possible the detection of damage with only the use of simple and inexpensive electrical equipment, leading to the development of a smart material. This capability is based on the assumption that the volume electrical resistivity of the composite depends on crack generation and propagation under stress. The combined use of IS and computer simulation showed that the presence of highly conductive, oriented fibers in a relatively poor-conducting matrix induces changes in the impedance spectrum that can be quantitatively associated with fiber length, orientation, and volume fraction. The main effect was the resistance at DC or low-frequency AC depended almost entirely on the matrix, while the resistance at high frequencies depended almost solely on the fiber properties and geometry. Using this frequency-dependent “separation” of fiber and matrix behavior, the crack propagation process of FRC has been studied (Torrents et al. 2001).

Torrents et al. (2000) investigated the correlation between electrical (DC and AC) and mechanical properties of cement composites reinforced with conductive carbon fibers. The tensile and impedance behavior of extruded and notched composites with fiber volume fractions of 0.5% and 3% were examined. Mechanical loads and an electrical field were applied, and crack growth during loading was analyzed by digital image correlation (DIC). Impedance Spectroscopy measurements were made under loaded and unloaded conditions to address the effect of specimen geometry, the manufacturing process, and the effect of fiber volume fraction.

Using these IS measurements, along with numerical computations, the bridging area of the fibers was extracted quantitatively from the tensile measurements. A good correlation between the electrical and mechanical properties was found when a sudden growth of the crack was observed; a dramatic change was also noticed in the impedance values.

Impedance measurements have been used along with the conventional mechanical tests for assessing damage under load in composites reinforced with conductive fibers. Taking advantage of the special frequency-dependent electrical properties of conductive FRC, impedance values measured during the fracture process were used to distinguish and calculate three different areas at the crack front: uncracked, bridging, and open areas. The bridging area is the zone where fibers bridge the propagating crack. A greater bridging area was found for the 0.5% fiber composite than for the 3% fiber composite, due to differences in the final length of the carbon fibers in both composites. The high content of fibers in the 3% fiber system increased the stiffness of the fresh mixture, leading to higher forces during mixing and extruding, which resulted in increased fiber breakage and shorter final length, as confirmed by optical microscopy (Peled et al. 2001).

The addition of carbon fibers to portland cement-based concrete decreases the bulk electrical resistivity. Reza et al. (2001, 2003, 2004) measured the electrical resistivity of carbon FRC specimens as a function of curing time. The dependence of this electrical resistivity on the water-cementitious material ratio (w/cm), sand-cement ratio, volume fraction of carbon fibers in the mixture, and the length of fibers was determined. Results indicate incorporation of carbon fibers in amounts as low as 0.5% by volume significantly decreased the bulk electrical resistivity of mortar. The four-ring electrode configuration was an effective method for measuring the volume electrical resistivity of concrete samples. The w/cm did not significantly affect the electrical resistivity in the presence of carbon fibers.

Alternating current power is preferred for measuring the electrical properties of FRC. Direct current power exhibits a voltage across the inner ring electrodes for several minutes after the power is turned off creating a polarization potential that reduces the voltage drop across the ring electrodes. A discussion of the polarization potential can be found in Monfore (1968) and Banthia et al. (1992), who both made electrical resistivity measurements of combinations of carbon and steel fiber-reinforced mortars. Niemuth (2004) used electrical impedance to detect and image cracking in concrete elements. The state of stress is related specifically to the electrical conductivity or volume resistivity of carbon fiber-reinforced mortar (CFRM). By applying an AC current in the frequency range of 20 Hz to 1 MHz, Nyquist plots were made of the imaginary part of the impedance, reactance, versus the real part of the impedance, resistance (Torrents et al. 2000).

Owing to a unique frequency-dependent behavior of conductive fibers, Woo et al. (2005) employed AC-IS to monitor various dispersion issues in steel fiber-reinforced, cement-based materials. First, AC-IS was used on model-scale specimens to understand the ability of the method for

monitoring various dispersion issues such as fiber clumping, fiber orientation, and segregation. Mathematical expressions based on an intrinsic conductivity approach were used to evaluate characteristics of fiber dispersion, and very good results were obtained (Douglas and Garboczi 1995). Next, AC-IS was compared with a conventional time- and labor-intensive image analysis (Özyurt et al. 2006a), and fiber clumping and fiber orientation were measured using AC-IS and image analysis. The results of the two methods were found to match well in experimental uncertainty. Later, model studies on small-scale specimens were extended to large-scale specimens. Fiber orientation in an industrial-scale beam was evaluated using AC-IS and image analysis (Özyurt et al. 2004), and both methods gave similar results. Finally, fiber segregation in cylindrical specimens was studied by obtaining AC-IS measurements along the height of cylinders (Özyurt et al. 2007). The results were successfully used to relate fresh state properties to fiber segregation. Woo et al. (2005) recently showed that measurements related to fiber dispersion monitoring can be extended to fresh-state fiber-reinforced materials. By using AC-IS with another electrical measurement technique (time domain reflectometry), they determined the parameters necessary for fiber dispersion analysis at early times (Özyurt et al. 2006b).

Current research activity on the use of AC-IS for non-destructive monitoring of fiber dispersion deals with the assessment of its applicability to real size structural elements, with the objective of implementing such a technique into quality control procedures at the industrial scale. The uniformity of dispersion as well as issues related to the orientation of fibers play a major role in the promotion of SFRC in full load-bearing structural elements. Within the broadest range of foreseeable applications, attention has been focused on thin web roof elements.

3.6—Thermal conductivity

Both transient (unsteady heat flow) and steady-state heat flow are used for measuring the thermal conductivity of materials. The transient heat flow or “probe” procedure is well suited for homogeneous materials, while the steady-state heat flow procedure is better suited to nonhomogeneous materials such as mortar and concrete. In the steady-state procedure, a linear heat flow is created and the thermal temperature gradient is measured.

Cook and Uher (1973) used blocks of FRC with a copper plug and a resistor inserted in a hole on the top surface and the bottom surface in contact with a water-cooled, copper heat sink. The fiber concrete blocks were 3 x 3 x 6 in. (75 x 75 x 150 mm) and made of a mortar or concrete mixture containing 0.0, 0.5, 1.0, 2.0, 4.0, and 8.0% volume of copper fibers or steel fibers, 0.003 in. (0.8 mm) in diameter and 1 in. (25 mm) long. Thermal conductivity measurements were compared with a mathematical model developed by Lakkad et al. (1972) that provided upper and lower bounds on the thermal conductivity. The thermal conductivity of the plain mortar was 0.862 W/m °C and that of the concrete was 1.530 W/m °C. Morel (1970) investigated concrete mixtures with 0.0, 0.5, 1.0, and 1.5% volume of steel fibers with two

Table 3.1—Thermal conductivity measurements of fiber-reinforced mortar by Morel (1970)

Fiber volume percent and fiber shape	Thermal conductivity, W/m°C
0.0	2.75
0.5 flat	2.67
1.0 flat	2.80
1.5 flat	3.03
0.5 crimped	3.03
1.0 crimped	2.74
1.5 crimped	2.84

Note: $1 \text{ W}\cdot\text{m}^{-1} \cdot\text{C}^{-1} = 0.578 \text{ BTU h}^{-1}\text{ft}^{-1}\text{F}^{-1}$.

different geometric shapes: flat and crimped. The concrete was a mortar with a w/cm of 0.60 and sand-cement ratio of 2.50. The thermal conductivity of the SFRC can be calculated by the following equation for steady-state conditions

$$K_u = K_s \frac{\Delta T_s}{\Delta T_u} \quad (3-4)$$

where K_u = unknown thermal conductivity; K_s = known thermal conductivity; ΔT_s = temperature difference through the thickness of the material with known thermal conductivity; and ΔT_u = temperature difference through the thickness of the material with the unknown thermal conductivity.

Any free moisture will change the thermal conductivity during the test; it will take several hours before the stack reaches steady-state conditions. Prior to testing, it is recommended to oven-dry the FRC at 302°F (150°C) until a constant weight is achieved (Thompson 1968). The thermal conductivity measurements in Table 3.1 are based on the average of three stacks of each fiber volume percentage for the two geometric fiber shapes in a mortar matrix.

The main difficulty associated with the steady heat flow procedure to measure thermal conductivity of concrete is moisture migration (Thompson 1968). A 10% increase in moisture can result in a 50% or more increase in thermal conductivity. The increase depends on the concrete porosity (diffusion coefficient) and water movement. The thermal conductivity of concrete depends on the aggregate type and ranges from limestone (3.1), sandstone (3.9), granite (3.1), and basalt (1.4) W/m °C that results in an approximate range of 1.4 to 3.9 W/m °C (Troxell et al. 1968).

The thermal conductivity data recorded by Cook and Uher (1973) and by Morel (1970) indicate that, although there are slight increases in thermal conductivity for paste and mortar containing steel fibers, the increase is less than the effect of coarse aggregate normally found in concrete.

CHAPTER 4—DURABILITY OF FRC

4.1—Extreme temperature and fire

Concrete is more resistant to extreme temperatures than wood and steel because it has a low thermal conductivity, high heat capacity, and does not fuel combustion when exposed to flames. Constituents such as cement clinker and certain aggregates tend to be chemically and mechanically stable at elevated temperatures. Other constituents, including

the main hydration products, are less resistant to high temperatures, and are affected by moisture loss, microcracking, and damage by differential expansion. Reinforcement in the form of steel fibers only, synthetic fibers only, or a hybrid of steel and synthetic fibers, generally improves the performance of structural concrete members under extreme temperature and fire. The number and variety of test and field studies supporting this observation, however, is limited.

Ordinary concrete loses a sizeable fraction of its strength when exposed to prolonged high temperatures. Generally at about 400°F (204°C), concrete degrades as the bond of the cement paste and aggregates deteriorates. At 800°F (427°C), normal concrete maintains only about 50% of its original compressive strength. Once the internal concrete temperature exceeds 1700°F (927°C), there is over 90% loss of the integrity of unrestrained concrete (Schneider 1983). Fiber additions will not prevent failure under such extreme conditions, but fibers have been successful in extending the safe time of fire exposure for many practical and proven applications. Extending the safe time of fire exposure allows fire fighters more time both to evacuate structures and to extinguish the fire safely.

Over the past several decades, there has been a steady trend toward using higher-strength concretes within the civil infrastructure. Densification of the concrete microstructure has also led to improvements in other important properties (for example, permeability and electrical resistivity), but the material has also become more vulnerable to brittle behavior during fire loading. Both material strength loss and the potential for spalling should be factored into design. The spalling of high-strength concrete (HSC) panels in the 1996 Channel Tunnel connecting France and England has drawn attention to the issue of HSC fire resistance (Ulm et al. 1999). Spalling, which at times may be explosive, is particularly worrisome due to the sudden, potentially large loss of cross-sectional area and the associated loss in load-carrying capacity of a structural component. Loss of protective cover also exposes reinforcing steel to higher temperatures. Fire studies show that in addition to member size, the effect of heat depends on several factors, including: temperature and duration of fire, rate of heat transfer (concrete material property), moisture content of concrete, specimen geometry, concrete age (meaning strength and temperature maturity), type of aggregates, and other factors.

Goldfein (1963) reported on the use of polymeric fibers for blast and impact resistance. Soon after, some of the first FRC concrete was used for missile silos and launching pads to enhance longevity by reducing the thermal shock, explosive spalling, and subsequent repairs at the fire-exposed surface.

In the 1970s, SFRC was used for crib blocks and tunnel supports in the mining industry to replace wooden timbers to minimize tunnel fires. Fire tests indicated that PP fibers melt when the temperature rises, causing the polymer to volatilize, leaving fine channels or capillary pores for relief of built-up steam pressure that left the concrete fully intact (Hannant 1978). In the late 1980s, hybrid combinations of steel and PP fibers were first used for precast concrete fireplace hearths, with little or no explosive spalling. Also in the 1980s,

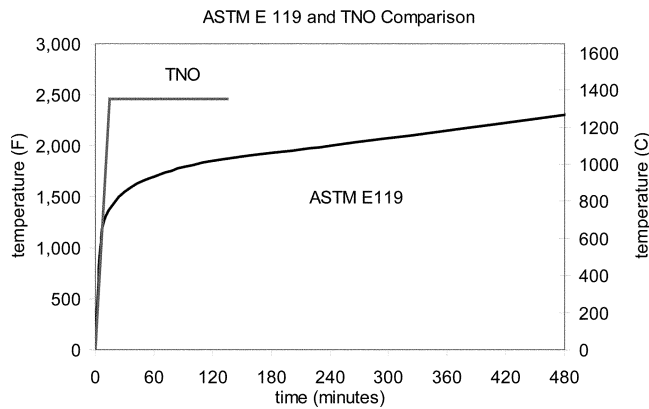


Fig. 4.1—ASTM E119 standard and TNO hydrocarbon fire curves (Hoff 1996; Moody et al. 2003).

Babcock and Wilcox patented the use of PP fibers for use in refractory applications. Studies of PP-FRC by Vondran (1989) and Schwein (1988) indicated 2- and 3-hour fire ratings are achievable for metal deck composites.

Hoff (1996) has compared the hydrocarbon fire time-temperature curves of Technical Centre for Fire Prevention, The Netherlands, (TNO) and ASTM E119, suggesting that the TNO curve is more likely to induce spalling. Because most concrete structures are approved in the permit phase of construction based on existing fire rating standards, designers should consider longer (4-hour) ratings or other fire requirements, especially where there is a potential risk of hydrocarbon-fueled fires that burn hotter and faster. Time-temperature curves are compared in Fig. 4.1.

ASTM E119 fire test standards, used mainly to determine the fire resistance of component assemblies and systems, are based on a slow temperature rise over 3 hours to reach 2000°F (1093°C), similar to a wood-burning fire exposure. Many hydrocarbon fueled fires, however, have a much faster temperature rise, about 15 minutes, to 2000°F (1093°C), which can cause catastrophic failure.

Recent studies by the Technical Research Centre of Finland (Holt 2003) evaluating self-consolidating concrete (SCC) cite Swedish studies (Bostrom 2002) that concluded that PP fibers greatly reduce the risk of spalling. A PP fiber dosage of 0.7 lb/yd³ (0.4 kg/m³) reduced both debris fallout and spalling. Effectiveness of PP fibers in reducing the risk of spalling depends not only on the volume content, but also on the length and diameter of the fibers. In general, fibers with small diameters (low-denier fibers) provide significantly better spalling resistance (Bilodeau et al. 2003).

As for spalling, there is typically excess water in concrete mixtures for workability or other transport, mixing, and batching issues. Most excess mixing water remains as free moisture in the pore structure of the hydrated cement paste. Moisture is also lost and gained through environmental exposure. When concrete is exposed to fire, the temperature increase may be sufficient to change interior free moisture into steam or vapor, creating pressure within the concrete. If there is no mechanism for pressure release, the internal pressure may exceed the tensile capacity of the concrete, causing spalling, which can be explosive in nature. England and

Khoylou (1995) have concluded that explosive spalling is strongly related to the amount of free water in the concrete and its distribution during heating. They also identified four specific water content zones in concrete subjected to fire: 1) dry or superheated steam; 2) partially saturated; 3) physically saturated; and 4) second partially saturated. The spalling damage can penetrate more than 6 in. (150 mm) into the concrete as layer after layer of concrete sloughs away or comes off the exposed face where the fire is incident to the concrete. Spalling is a major concern because the loss of concrete cover may compromise the load-carrying capacity of structural elements. As the concrete cover spalls and falls off, underlying reinforcing steel can be exposed to high temperature, rapidly deteriorating its ability to carry load. Building fires may initially be less intense as they begin slowly, unlike a hydrocarbon fire that is instantly intense. Significant surface spalling problems have occurred when concrete airfield surfaces are subjected to streams of hot jet exhaust (Schwein 1988). Polypropylene fibers smaller than 33 μm in diameter and generally less than 0.5 in. (12 mm) long can significantly reduce spalling (Tatnall 2002).

Fibers are used to improve the fire resistance of concrete in several ways, including increasing residual strength and toughness and preventing explosive spalling. The first case involves the rather classic application of short-fiber reinforcement to bridge cracks to maintain integrity of the damaged material. Steel fibers have been useful in maintaining residual strength after high temperature loading, but high volume fractions (on the order of 2%) are needed (Gambarova 2004). Di Prisco et al. (2003) found that the presence of steel fibers enhanced fire resistance of small-scale concrete slabs. Slabs with steel fibers endured fire loading three to nine times longer than control specimens without fibers.

ACI 216.1 provides code requirements for determining the fire endurance of several types of concrete members, based mostly on studies of NSC members. The addition of polymeric materials such as PP fibers appears to be the most effective method in preventing explosive spalling (Dehn and König 2003; Chandra et al. 1980; Ali et al. 1997; Bentz 2000; Bilodeau et al. 2004). The low melting point (about 220°F [160°C]) of PP and its decomposition at higher temperatures provides channels for pore pressure release. Effectiveness depends on size, distribution, and volume content of PP fibers. Table 4.1 summarizes some of the conditions that aggravate fire-induced spalling and the mechanisms by which PP fibers help mitigate such spalling. PP fibers have very different thermal expansion properties than HSC and, thus, even before they melt, discontinuities between the fibers and the matrix form and allow dissipation of vapor pressures (Tatnall 2002).

Low volume fractions of PP fibers (0.2 to 0.5%) can achieve percolation within HSC, whereas in NSC the relatively larger interfacial transition zones between the aggregates and the matrix may provide the necessary channels for pressure relief. According to the literature, 3.3 lb/yd³ (2 kg/m³) of PP fibers are typically added to HSC to prevent explosive spalling (Kalifa et al. 2000; Garboczi et al. 1995; Velasco et al. 2004).

Table 4.1—Conditions that aggravate fire-induced spalling and the role of PP fibers (Hoff 1996)

Conditions that aggravate fire spalling	Role of PP fibers in spall mitigation
<ul style="list-style-type: none"> • High-strength concrete • Poor-quality aggregate • Dense concrete matrix • Exposure to fire on only one side • Service loads • High moisture content and its migration in the concrete • Rapid increase in heat such as due to hydrocarbon-fueled fires • Duration of fire 	<ul style="list-style-type: none"> • Polypropylene melts at 150 to 220°F (140 to 160°C) • 99% of fiber is lost on ignition • Voids left by fibers act as pore space • Venting out the voids creates micro geysers as internal temperatures rise • Steam has a path of escape without the pressure exceeding the tensile strength of concrete and therefore causing damage to the concrete

Polypropylene fibers have been used in the final shotcrete lining of the Weehawken Tunnel in New Jersey (Garret 2004), in the precast segmental linings of the Channel Tunnel Rail Link tunnels (Tatnall 2002), the Dartford Cable Tunnel (Craig 2004) in the UK, and the Malmö City Tunnel project in Sweden (Craig 2006) for resistance to explosive spalling in fires.

4.2—Freezing and thawing

Most of the durability studies conducted to date on FRC have focused on the corrosion resistance of steel fibers. Little published information currently exists on the effects of fiber reinforcement on the freezing-and-thawing resistance of concrete. Of particular interest is the determination of the major factors that may affect the durability of FRC under freezing-and-thawing conditions including air content, cement content, *w/c*, fiber type, fiber content, and geometry. Section 4.2.1 provides a summary of key research findings on the freezing-and-thawing resistance of steel, synthetic, and cellulose FRC.

4.2.1 Steel fibers—Balaguru and Ramakrishnan (1986) examined the effects of varying parameters of air content, cement content, fiber content, and *w/c* on the freezing-and-thawing resistance of SFRC. Air contents varied from 1.2 to 10.8%. Cement contents of 611, 690, and 799 lb/yd³ (362, 408, and 473 kg/m³) and steel fiber (hooked-ends) contents of 75 and 100 lb/yd³ (44.4 and 59.2 kg/m³) were used. The freezing-and-thawing test was conducted according to ASTM C666/C666M, Procedure A. For each mixture prepared, two 4 x 4 x 14 in. (100 x 100 x 350 mm) beams were subjected to more than 300 freezing-and-thawing cycles. Results indicate that air content is the most significant factor for the freezing-and-thawing resistance of SFRC. Like plain concrete, the addition of entrained air improves the freezing-and-thawing resistance of SFRC. The same air content and freezing-and-thawing resistance is found in both plain and steel fiber-reinforced concrete. The rupture modulus of the beam specimens decreased with freezing-and-thawing cycling for both plain and SFRC. The reduction was smaller for SFRC than for plain concrete. Reductions in flexural strength of SFRC and synthetic FRC with freezing-and-thawing cycles have also been investigated (Trottier et al. 1996; Trottier and Forgeron 2001; Forgeron and Trottier 2004). The

authors concluded that all specimens tested (synthetic and steel fiber-reinforced concrete) had excellent resistance to freezing and thawing as measured under ASTM C666/C666M, Procedure A.

Rider and Heidersbach (1980) also examined the freezing-and-thawing resistance of FRC. Four hundred cycles of freezing and thawing were conducted on a series of air-entrained SFRC specimens and their controls. No measurable degradation occurred in the specimens. They summarized their findings by recommending that the mixture design for SFRC, which has to be used in a marine environment, should have a *w/c* of not more than 0.45 (by weight), a minimum cement content of 865 lb/yd³ (519 kg/m³), and air contents from 6 to 7.5%.

Results were obtained by Ishida et al. (1985) on the freezing-and-thawing resistance of steel fiber-reinforced lightweight-aggregate concrete. Increasing fiber content in the range of 0.5% to 1% by volume steel fiber did not show a remarkable improvement of the freezing-and-thawing resistance of lightweight-aggregate concrete.

Different conclusions from the general trends discussed above have been reported by Kobayashi (1983). The results are not much different for ordinary concrete, when air is not entrained. For air-entrained concrete (with air content 5 to 6%), there is a marked improvement for FRC compared with ordinary concrete.

4.2.2 Synthetic fibers—Limited research has been conducted on the freezing-and-thawing resistance of synthetic FRC. Vondran (1987) reported that synthetic fiber reinforcement improves freezing-and-thawing resistance of concrete (ASTM C666/C666M, Procedure A) and deicer scaling (ASTM C672/C672M). Test results indicate PP fiber-reinforced slabs had less scaling at 50 cycles than non-fibrous reference slabs at 35 cycles. Both lab tests concluded that the proper amount of air entrainment is necessary for durability.

The effect of low-dosage PP microfiber-reinforced air-entrained cementitious grouts was investigated by Allan and Kukacha (1995). The fibers used were 0.75 in. (19 mm) long collated, fibrillated fibers at a relatively low volume fraction of 0.1 and 0.2%. Resistance of the unreinforced and fiber-reinforced specimens to freezing-and-thawing cycles was assessed using ASTM C666/C666M, Procedure A. The authors concluded that the fibrillated PP fibers had no influence on the freezing-and-thawing resistance of the grouts and that such fibers are unlikely to substitute for air entrainment in said materials. Berke and Dallaire (1994) also found similar trends with air-entrained concretes reinforced by similar fiber types and fiber dosages.

The freezing-and-thawing resistance of macro-synthetic (polyolefin) FRC was investigated by Trottier and Forgeron (2001). The polyolefin macrofiber was added at a dosage rate of 25 lb/yd³ (15 kg/m³) or 1.67% by volume. As in the case of steel fibers, the freezing-and-thawing cycling caused a 15% reduction in the flexural strength of the polyolefin FRC compared to 30% for the plain concrete specimens. The flexural stiffness of the plain samples was reduced by 32% compared to only 13% for polyolefin FRC.

Unlike steel fibers, the flexural toughness of the polyolefin FRC samples subjected to freezing and thawing was reduced by 17% as compared to control samples tested at the age of 90 days.

4.2.3 Cellulose fibers—Fiber-reinforced cement board (FRCB) is a laminated material composed of cellulose fibers (9% by weight), cement, silica, and water. It is produced by the Hatschek process and is currently used in the North American building materials industry. Fiber-reinforced cement board is susceptible to freezing-and-thawing degradation because of its high porosity, the hydrophilic nature and tubular structure of the cellulose fibers, and the laminated structure of the composite. Kuder and Shah (2003) reported the effect of pressing the material after it is formed on freezing-and-thawing resistance of FRCB. Commercially-produced FRCB with four different pressure treatments ranging between 0 and 30 bars (3 MPa [435 psi]) were tested to assess flexural strength and inter-laminar bond (ILB). Specimens were subjected to 300 accelerated freezing-and-thawing cycles according to a modified version of ASTM C1185. It was concluded that pressure treatment improves the freezing-and-thawing ILB strength, but does not affect flexural strength or porosity.

4.3—Degradation and embrittlement due to alkali attack and bundle effect

Many fiber types such as glass, polymeric, and natural fibers lose strength in the long term as a consequence of weathering. Knowledge of this time-dependant development of strength and ductility loss is an essential aspect for the application of fiber-reinforced components in structurally relevant areas. Section 4.3.1 addresses various degradation mechanisms in different fiber systems.

4.3.1 Glass fibers—Glass fiber-reinforced concrete (GFRC) is probably the most studied cement composite, particularly for its durability. Glass fiber-reinforced concrete typically contains alkali-resistant (AR) glass fibers between 3% and 5% of the total composite weight. This makes it a very different material from all the other FRC materials discussed in this report, which typically have low fiber dosages of less than 1.5% by volume. When AR glass fibers are used in contents less than 3% by weight, there is little evidence of strength reduction; in fact, strengths are stable with time. The change in properties with time of GFRC composite has been known even before GFRC became commercially available. Glass fiber-reinforced concrete has been widely and successfully used all over the world for over 35 years because a design methodology based on durability was established at the beginning that took account of the long-term properties of GFRC. This has resulted in no demonstrated product failures from durability issues in the GFRC.

Over 90% of the GFRC in existence around the world is based on the original formulation using portland cement without the addition of the property enhancement materials such as blended cements. This is not to say these additives do not add benefit in certain circumstances but conventional ordinary portland cement (OPC)-based GFRC has proved to be a very durable building material for many products such as various architectural panels, utility products, roofing

products, portable buildings, artificial rockwork, highway noise barriers, agricultural products, and many other products.

The first GFRC has been credited to Biryukovich et al. (1957, 1961) who combined portland cement with E-glass fibers used for electrical insulation, a borosilicate glass formulation used for plastics. Standard glass formulations, however, suffer severe corrosion and strength loss in the highly alkaline environments. Building Research Establishment (BRE) and Pilkington Brothers Ltd. carried out investigations and evaluations of various AR glass fiber compositions, which led to the selection of a sodium-zirconium-silicate glass. Development of GFRC would not have been possible without the design of AR glass, which became commercially available in 1971.

Glass fiber-reinforced concrete shows a reduction in properties such as strength, ductility, toughness, and impact resistance over time. Durability of GFRC was documented by Majumdar and Laws (1991). Assuming that fiber corrosion was the main degradation mechanism, accelerated aging procedures were developed to predict the long-term strength of the composite. The “strand in cement” (SIC) test was developed, where a single strand was encased in a cement paste prism and then aged in hot water at various temperatures before testing to failure (Litherland et al. 1981). The accelerated aging tests were then compared with 10-year, real-life weathering data and based on the comparison of empirical relationships between accelerated aging regimes. A range of temperatures between 41 and 176°F (5 and 80°C) and real weathering acceleration factors used (Aindow et al. 1984; Litherland 1986; Proctor et al. 1982). Based on the model, a table including the relationship between time in accelerated aging (different temperatures) and exposure to real weathering was proposed (Proctor et al. 1982) and used as a basis for testing GFRC products ever since.

Investigations concerning GFRC durability were initiated; it was established that AR-glass GFRC properties are reduced by more complex mechanisms than the glass-fiber corrosion behavior, which is dominant in E-glass fiber GFRC. Scanning electron microscopy (SEM) studies of GFRC microstructure identified two degradation mechanisms: densification of the fiber-cement interface with time, and filling space between the filaments in a strand by $\text{Ca}(\text{OH})_2$, reducing the strand's flexibility (Bentur and Diamond 1984; Bentur 1986).

The agent responsible in most cases was calcium hydroxide (portlandite), a product of cement hydration. In addition to strength loss, a reduction in strain capacity and total ductility of GFRC composites was also noted (Shah et al. 1988; Mobasher and Shah 1989). Identifying two degradation mechanisms directed GFRC development toward modified matrixes and fibers in view of obtaining improved long-term durability. Matrix modifications were aimed to reduce the amount of portlandite produced during cement hydration, either by using ingredients/additives such as ground-granulated blast-furnace slag, silica fume (Kumar and Roy 1985), fly ash (Leonard and Bentur 1984), or non-ordinary portland cement matrixes, particularly those based on calcium aluminates or sulfo-aluminates (Litherland and Proctor 1986). Blended cement ingredients such as metakaolin

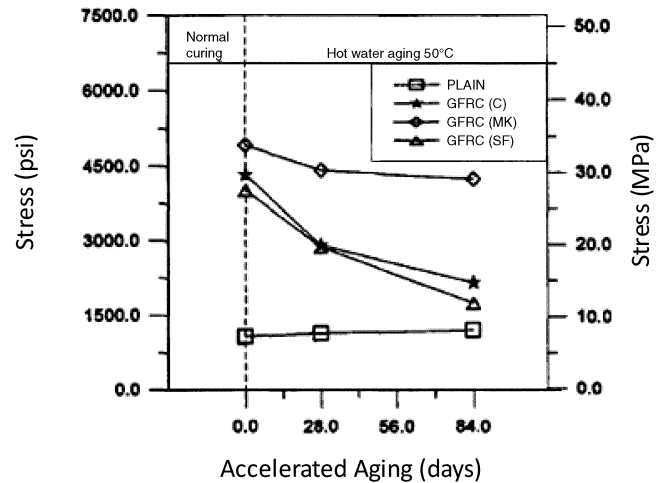
(Marikunte et al. 1997; Beddows and Purnell 2003; Purnell and Beddows 2005) have been used. Acrylic polymers are routinely used for GFRC production for durability improvement and curing aid (Bijen 1983, 1986; Ball 2003). New cement formulations such as sulfo-aluminate cement (SAC) (Qi and Tianyou 2003; Ambroise and Péra 2005; Litherland et al. 1981; Gartshore et al. 1991), inorganic phosphate cement (IPC) (Cuypers et al. 2000, 2003, 2005, 2006) and calcium aluminate cement (CAC) (Brameshuber and Brockmann 2001a,b) have been investigated in terms of their effects in improving GFRC long-term durability. Figure 4.2 shows comparison results of flexural strength decay.

Ambroise and Péra (2005) concluded that GFRC using AR-glass and calcium sulfo-aluminate (CSA) cements were more durable than Type I and II cements. Cuypers et al. (2000, 2003, 2005) reported that inorganic portland cement (IPC) GFRC property retention is better for both E- and AR-GFRC compared with AR-glass OPC GFRC. Marikunte et al. (1997) studied the hot-water durability of AR-glass fiber-reinforced composites in a blended cement matrix and rated them for their flexural and tensile performance. The different matrixes selected were: a) cement; b) cement + 25% metakaolin; and c) cement + 25% silica fume. Specimens after normal curing of 28 days were immersed in a hot water bath at 122°F (50°C) for up to 84 days and then tested in flexure and tension. The blended cement consisting of metakaolin significantly improves the durability of the GFRC composite (Fig. 4.2). Beddows and Purnell (2003) and Purnell and Beddows (2005) used more than 1100 aged GFRC samples for the development of a durability model, including OPC I and OPC II, and GFRC with metakaolin, polymers, and sulfo-aluminates (44% of the data available from literature, 25% from industry, 28% generated) and concluded that AR-glass composites with OPC + 5% polymer + a proprietary cement with sulfo-aluminate-based additives were the most durable of the GFRCs tested (Fig. 4.3).

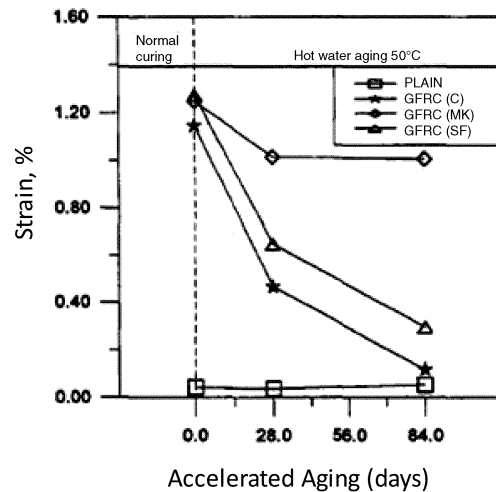
4.3.1.1 Glass fiber-reinforced concrete damage mechanisms identified are:

4.3.1.1.1 Chemical attack—Glass is chemically attacked by hydration products (hydroxyl ions), leading to a breakup of the Si-O-Si glass network, which leads to a weak glass surface. Initially, the corrosion rate is linear with time, but the process slows down with increasing zirconium concentration in the deeper layer and becomes diffusion controlled. Orlovsky et al. (2005) proposed a model based on physico-chemical degradation, which is based on chemical attack of the glass surface, resulting in defects and flaw growth without application of any mechanical load (rather than delayed fracture). Chemical attack occurs at various pH values, higher for high pH and lower for low pH.

4.3.1.1.2 Mechanical attack—Formation of hydration products in the interface zone of a glass fiber concrete may increase transversal shearing on the filament and lead to embrittlement (loss of ductility). Embrittlement from growth of hydration products around glass filaments, particularly Ca (OH)₂ crystals, occurs at an early stage of composite curing, which leads to loss of filament strength before the



(a)



(b)

Fig. 4.2—(a) Flexural stress; and (b) strain at failure (modulus of rupture) (Marikunte et al. 1997).

chemical attack (Bentur 1984; Bentur and Diamond 1984; Majumdar and Laws 1991).

4.3.1.1.3 Delayed fracture—Delayed fracture occurs under static load due to the introduction of small defects in the production process. Purnell and Beddows (2005) developed a model based on the assumption that static fatigue of the fibers is responsible for the degradation observed in the material over time. Static fatigue is a delayed fracture phenomenon observed in glass. Under stress concentrations due to a constant load or a deposit of hydration products, surface flaws or defects start to grow, accelerate, and eventually lead to delayed fracture, which will depend on the mechanical load and environmental conditions, such as temperature, moisture, and pH. According to Purnell’s model, the strength loss with time for GFRC is expressed as

$$s = \frac{1}{\sqrt{1 + kt}} \tag{4-1}$$

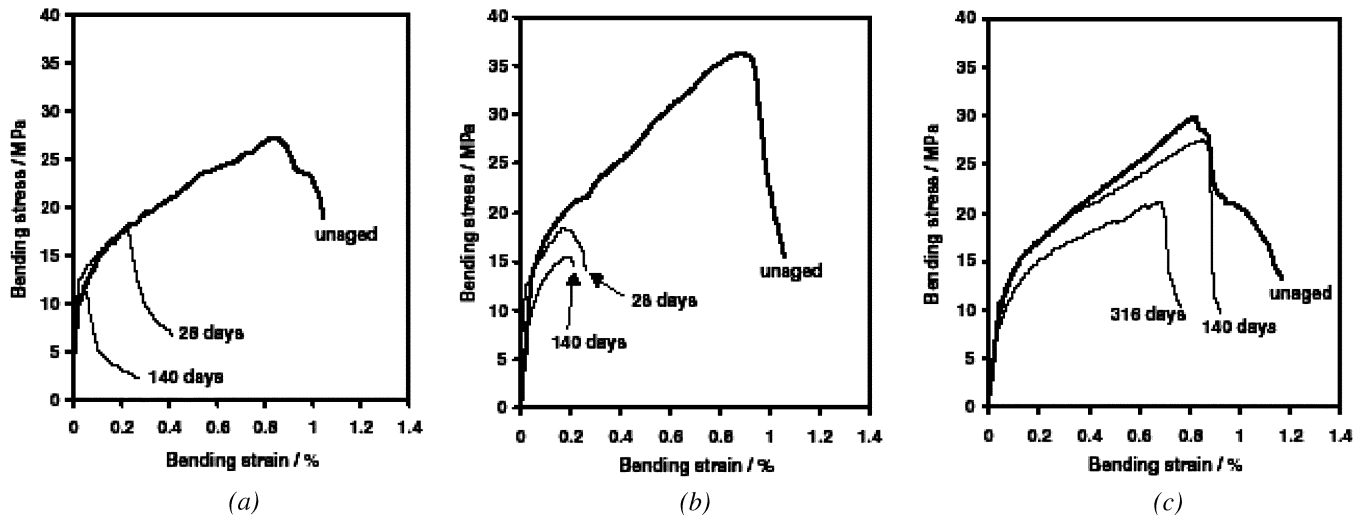


Fig. 4.3—Evolution of stress-strain curves for: (a) OPC II; (b) Poly II; and (c) Nash II composites aged at 122°F (50°C) (Purnell and Beddows 2005).

Table 4.2—Comparison of acceleration factors advanced by Litherland et al. (1981) and by Beddows and Purnell (2003)

	Aging regime	Strength fallen to percent of original	Equivalence using Litherland acceleration factors, years	Equivalence using new model acceleration factors, years	Time to reach same strength loss through natural weathering, years
GRC	32 days at 122°F (50°C)	70	8.8	10.7	10
OPC II	32 days at 122°F (50°C)	90	8.8	3	3
M II	90 days at 122°F (50°C)	80	2.5	8.3	7

$$k = k_o \exp\left(\frac{\Delta G}{RT}\right) \quad (4-2)$$

where s is the normalized strength, defined as the strength at time t divided by the original unaged strength; k is the reaction rate of the corrosion responsible for strength loss; ΔG is the activation energy required for the reaction to take place; k_o is the “frequency factor” of collisions between the reactants; T is temperature in Kelvin, and R is the universal gas constant.

Beddows and Purnell (2003) present a comparison of acceleration factors advanced by Litherland et al. (1981) and Purnell’s model for OPC II and M II (matrix modified with metakaolin) (Table 4.2). Litherland’s model can be used to estimate service life for OPC II, but it over-estimates service life for modified matrix formulations, whereas Purnell’s model can be used both for OPC and modified matrix formulations.

Options available to improve long-term durability of GFRc are:

- Using lower-alkalinity cement such as SAC, high-alumina cement (HAC), CAC, or IPC;
- Using ingredients/admixtures in the matrix to reduce the pH of the matrix, to react with the hydration products, to improve the chemistry of the pore solution and the interface fiber-matrix. These ingredients include silica fume, ground-granulated blast-furnace slag, metakaolin, and acrylic polymer; and
- Improving glass fibers by improving sizing chemistry or a polymeric coating to protect E- or AR-glass.

Far fewer $\text{Ca}(\text{OH})_2$ crystals precipitate in fiber bundles in non-OPC GFRc (Majumdar and Laws 1991). Sulfo-aluminate-modified cements (Nashrin-type) produce little, if any, $\text{Ca}(\text{OH})_2$. In metakaolin-type matrixes, $\text{Ca}(\text{OH})_2$ content is decreased (Purnell et al. 1999) and the $\text{Ca}(\text{OH})_2$ tends to precipitate away from the fibers. Fiber pushout tests and microstructural studies have shown that densification within the fiber bundle does not occur with aging in GFRc and metakaolin-modified GFRc (Zhu and Bartos 1997). Accelerated aging tests show both composites have improved durability compared with traditional OPC GFRc. Strength loss still occurs, however, although to a lesser extent (Marikunte et al. 1997; Zhu and Bartos 1997).

4.3.2 Cellulose fibers—Concerns over health issues resulting from the use of asbestos fibers in commercial production of cementitious products forced the industry to investigate and find safer reinforcing materials. In the 1970s, cellulose fibers were successfully experimented as a replacement for asbestos fibers in the industrial production of thin sheet products (ACI 549.2R).

In North America, cellulose-based FRC has found increasing applications in residential housing nonstructural components, such as siding, roofing, flat panel applications including underlayment, and tile backerboard and lumber substitutes such as trim, fascia, and corner boards. Cellulose-based FRC products have seen limited use in exterior applications due to degradation from ambient wetting and drying. Vegetable fibers is a generic term for a range of materials and can refer to fibers of any size, from particulate

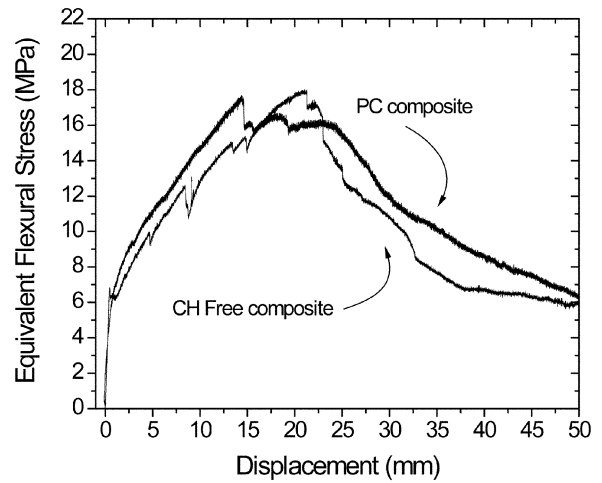
to long strands, which trace their beginning from a natural feedstock, such as pulp (cellulose), agave (sisal), coconut, hemp, flax, jute, or kenaf, rather than fibers consisting of a man-made material.

Several studies have been performed to examine the durability of cellulose-based FRC. They can be divided by reinforcement type: long fibers (Silva et al. 2006b), short fibers (Guimarães 1990; John et al. 1990) and pulp fibers (Mohr et al. 2005a,b, 2006; Soroushian and Marikunte 1992; Kim et al. 1999; Bentur and Akers 1989). A diversity of aging tests has been proposed and used: wetting and drying cycles, hot-water immersion, natural weathering, and modifications of the wetting and drying cycles. Researchers have developed a method consisting of storing the composites in a controlled wet climate (Gram 1988; Bergstrom and Gram 1984). Water maintained at a temperature of 50°F (10°C) is sprayed into the cubicle during a 30-minute cycle. This is followed by a heating cycle where the temperature reaches 221°F (105°C) for 5.5 hours before the process is repeated. Silva et al. (2006b) has developed the Forced Air Flow Chamber (FAFC), a piece of equipment that allows simulating the wind velocity and temperature of the drying process within the wetting-and-drying cycles. Degradation studies on the fiber done by submitting them to different alkaline solutions (Ramakrishna and Sundararajan 2004), and investigations on the composite pore water as well as the lignin content of the fiber before and after aging (John et al. 2005) have also been performed.

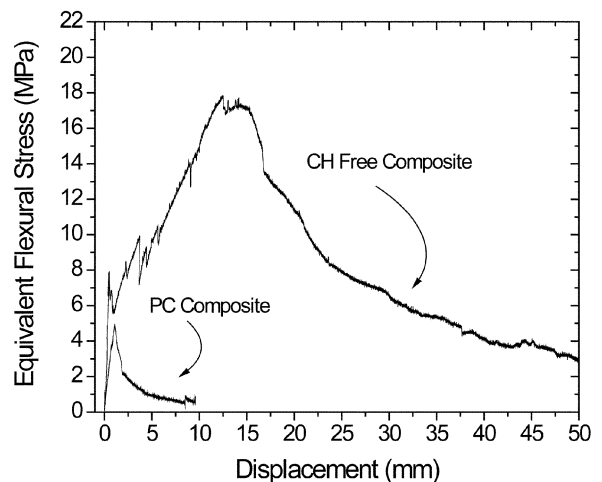
Several approaches to enhance the durability performance of cellulose-based FRC have been studied, including fiber impregnation with blocking agents and water-repellent agents, sealing the matrix pore system, reducing the matrix alkalinity, and combinations of fiber impregnation and matrix modification. One of the first and more comprehensive works dealing with the improvement of natural fibers' durability in cementitious matrixes was performed by Gram (1988).

Canovas et al. (1990, 1992) investigated impregnations of sisal fiber with timber-derived organic compounds such as tannins, colophony, and vegetable oils. Test results indicated a slowdown of the sisal fibers embrittlement process. Pore sealing with colophony, tannin, and montan was also investigated by Canovas and colleagues. Results indicated the water absorption and relative porosity of sisal fiber cement-based composites slowed its embrittlement process.

Toledo Filho et al. (2000b, 2003) attempted to overcome the durability problem of sisal fibers as reinforcement in an OPC matrix. The techniques used in this research were carbonation of the matrix, immersion of sisal fibers in a slurry of silica fume, and partial replacement of OPC by silica fume and blast-furnace slag. The cement replacement of 40% (by mass) by slag did not reduce the composite embrittlement. The addition of 10% of silica fume was effective to slow down the strength loss and embrittlement of the sisal fiber-reinforced cementitious composites. Toledo Filho's results agree with the results obtained by Gram (1988). Immersion of sisal fiber in silica fume slurry and carbonation also presented a promising alternative for increasing the durability.



(a)



(b)

Fig. 4.4—Typical four-point bending test curves of portland cement and calcium hydroxide (CH) free composites: (a) fog cured for 180 days; and (b) subjected to 25 cycles of wetting and drying after fog cured for 180 days (Silva et al. 2006a).

Silva et al. (2006a) proposed that the main degradation process was the precipitation of calcium in the middle lamella of the sisal fiber as well as in the fiber lumens. This calcium would come from the dissolution of calcium hydroxide. To overcome the degradation process, Silva and coworkers developed a matrix free of calcium hydroxide by replacing 50% of cement (PC) (composed with filler—in mass: 85% <clinker < 91%; 3% < gypsum < 5%; 6% < filler < 10%) by 30% of metakaolin and 20% of calcined waste crushed clay brick. Wetting and drying cycles were performed. Figure 4.4 shows that 25 wetting-and-drying cycles (each cycle corresponds to 24 hours of wetting and 48 hours of drying) did not decrease the ultimate strength and toughness of the CH-free composite (Silva et al. 2006a).

Long aligned fibers used as reinforcement appears to be a good alternative for developing durable composites. When randomly dispersed pulp and short fibers are used, some fibers will take bending loads in addition to direct tension.

Aged natural fibers have a much lower resistance to bending than to tensile loads. Matrix modification appears to be a much better alternative than fiber treatment. Calcium hydroxide-free matrixes show to be a promising alternative to develop durable cellulose-based FRC, as shown in Silva et al. (2006a).

4.3.2.1 Related mechanisms that lead to composite degradation during wetting-and-drying cycling have been identified as:

4.3.2.1.1 *Changes in degree of fiber-cement bonding*—Mohr et al. (2006) concluded that when softwood kraft pulp fibers are used, the majority of losses in composite strength and toughness occur early in the accelerated aging process due to increased fiber-cement bond. The mechanism for this early increase in fiber-cement bond is unknown; however, it is believed that this is due to lime formation or ettringite densifying the transition zone around the fibers. Toledo Filho et al. (2000b) and Savastano et al. (2001) identified the transport of hydration products, mainly lime, within the fiber's lumen and around the fibers during accelerated aging, as resulting in a decrease in interface porosity, which may be responsible for the increase in fiber-cement bond and the decrease in composite ductility.

4.3.2.1.2 *Fiber mineralization*—Bentur and Akers (1989) suggested that embrittlement of the fibers is caused by penetration of cement hydration products within the fiber, and Mohr et al. (2006) proposed that the embrittlement of the fibers occurs after the increase in fiber-cement bond.

Cellulose-based FRC undergoes an aging process leading to a reduction in mechanical properties, which is due to a weakening of the fibers by alkali attack, fiber mineralization due to migration of hydration products to the fiber lumens and to the fiber middle lamella, and volume variation in the fibers due to their high water absorption. ACI 549.2R presents research results including some durability aspects explaining the failure mechanism.

Cellulose is known as the most alkali-resistant component of pulp fibers, and fiber pulping processes have an effect on fiber durability due to the amount of lignin, hemi-cellulose, and cellulose content remaining following the process. Kraft pulp fibers obtained by chemical or kraft processes are more resistant than thermo-mechanically obtained fibers, which have lower cellulose and a higher lignin and hemi-cellulose content.

The effects of matrix composition have also been studied relative to the long-term performance of cellulose-based FRC. Toledo Filho et al. (2003) used silica fume as much as 30% and 40% slag as supplementary cementing materials to consume the calcium hydroxide. They concluded that silica fume significantly improves wetting-and-drying cycling performance, whereas slag has little effect on sisal fiber mortar composite durability. Toledo Filho et al. (2000a) investigated the effect of carbonation of the matrix and the immersion of sisal fibers in slurry silica fume prior to the fibers being incorporated in the portland cement mixture on durability of the composite.

ACI 544.1R has identified research needs in understanding the mechanisms where moisture and aggressive environments

change failure mechanisms and the refinement of cementitious matrixes to improve durability characteristics.

According to Silva et al. (2006a), options are available to improve long-term durability of vegetable fibers:

- Fiber impregnation with blocking agents and water-repellent agents;
- Sealing of the matrix pore system;
- Reduction of $\text{Ca}(\text{OH})_2$ content in the matrix; and
- A combination of fiber impregnation and matrix modification.

4.3.3 *Approaches for modeling and design of materials with aging characteristics*—After prolonged exposure to a wet climate, the strength of the FRC is reduced substantially, depending on the fiber type. To account for this eventual strength loss, GFRC panels are not considered suitable as vertical load-carrying components or as part of the lateral load-resisting system. The recommended practice for GFRC developed by the PCI Committee on Glass Fiber-Reinforced Concrete Panels (1981) assumes that the aged flexural (or tensile) ultimate strength of GFRC is equal to its 28-day proportional elastic-limit strength, which is essentially equal to the 28-day flexural strength of an unreinforced panel. In addition to a reduction in strength, GFRC composites can also show a drastic reduction in ductility because the peak tensile strain is reduced to a value corresponding to nearly that of an unreinforced matrix. The use of polymers in the matrix has been an effective means of reducing the degradation rate (Ball 2002, 2003; Bijen 1990; Bijen and Jacobs 1981). Recent results, however, may indicate that such reduction factors may be too conservative, and the results based on an accelerated aging test may be too severe considering the long-term performance test results obtained recently with blended cement matrixes.

Modeling the strength degradation rate depends on many factors, including reduction of glass strength and an increase in the bonding strength of the glass-to-matrix interface. Under these two conditions, the frictional pullout mechanism of fibers is replaced by fiber fracture, leading to an inefficient toughening of the composite when the energy-absorbing mechanism of pullout is replaced by fiber fracture. The effect of accelerated aging on the pullout response was studied by Li et al. (1990). Mobasher (2000) developed a model representing the aging in GFRC that is based on a combination of a fiber pullout model and a toughening model of fibers.

4.4—Weathering and scaling

The literature available on the resistance of FRC to deicer salt scaling is even more limited than what is available on the freezing-and-thawing resistance. Despite recent progress in concrete technology, the basic mechanisms of deicer salt scaling are still not perfectly understood even for conventional concrete. It is clear, however, that this phenomenon only affects a surface layer of a few millimeters, and the microstructure of this layer can be different than the bulk of the concrete. Fibers can be expected to influence scaling indirectly, mostly through their negative effect on workability. The presence of fibers generally requires the use of higher dosages

of admixtures and can make the finishing operations more difficult. In turn, these can affect the microstructure of the surface layers that control the deicer salt scaling resistance.

An extensive experimental program was carried out by Cantin and Pigeon (1996) to assess the resistance of SFRC to deicing chemicals. The basic parameters of the study were the quality of the air-void network, the water-binder ratio, the presence of silica fume, and the fiber types. They concluded that neither the presence of fibers nor their type had any significant influence on the scaling resistance.

Sanjuán et al. (1997) studied the effect of initial shrinkage cracks in the presence of fibers on the corrosion behavior of concrete. The advantage of fiber reinforcement was evaluated in terms of its influence on the corrosion of steel placed in the concrete. Mortar specimens with reinforcing bars were exposed to restrained shrinkage conditions by drying immediately after casting. Some of the matrixes were reinforced with low-volume PP fibers. After the initial curing, the specimens were held in a corrosive condition by placing them in contact with chloride solutions, and the corrosion rate of the bars was monitored by electrochemical means and visual observations of crack development. The general trends between the various specimens tested were addressed. It could be concluded that, for systems of the same matrix composition, those with fibers seemed to crack less initially and later had somewhat lower corrosion rates as measured by the linear polarization method.

In their investigation on the salt scaling resistance of SFRC as per ASTM C672/C672M, Trottier et al. (1996) reached different conclusions. Scaling on the plain concrete specimens was much more pronounced (rating of 5 as per ASTM C672/C672M [severe scaling]) (coarse aggregate visible over entire surface) than that of the SFRC specimens (average rating of 4 as per ASTM C672/C672M [moderate to severe scaling]).

Ramakrishnan and Coyle (1986) reported some rusting of the steel fibers exposed by the scaled concrete at the end of 50 cycles of exposure to deicing chemicals. The higher-cement-content, lower-water-cement-ratio concrete experienced no scaling at the air contents tested (two batches at 6.0 and 3.9%). The lower-cement-content, higher-water-cement-ratio concrete showed slight scaling at the air contents tested (two batches at 7.8 and 7.4%).

Schupack (1985) initiated a study that exposed steel fiber-reinforced lightweight-aggregate concrete to the tidal zone of Long Island Sound in Norwalk, CT. The specimens were placed approximately at mid-tide, while some of the specimens were partially inserted into the highly organic marsh silt. No measurements were made to determine the actual cycles of freezing and thawing for specimens located at mid-tide, but it was estimated at 30 to 50 cycles per year. Schupack observed no freezing-and-thawing damage after approximately 10 years of exposure for air-entrained SFRC. Surface conditions were aesthetically affected by surface corrosion (staining) of the steel fibers, but no significant deterioration in material resulted. A review of a variety of investigations on the durability of FRC in severe marine environment was conducted by Hoff (1987).

4.5—Corrosion resistance

For conventionally reinforced concrete, codes of practice specify stringent cover requirements for the reinforcing bars, in part to guard against reinforcement corrosion. For SFRC, some of the randomly and uniformly distributed fibers in the matrix actually lie at the surface of concrete and are not protected from the surrounding environment by any concrete cover. This inevitable zero cover has led several researchers and potential users to mistakenly think that rapid and extensive corrosion of steel fibers would occur, especially fibers at or very near the surface and when the concrete is cracked in service.

The primary causes of corrosion in conventionally reinforced concrete apply equally to SFRC. These are chloride-induced corrosion and corrosion caused by the reduction of pH of the concrete matrix from carbonation. The availability of oxygen and moisture is essential to sustain the corrosion processes. Threshold levels of chloride ion concentration, which cause depassivation of steel reinforcement in concrete, have been established to be in the range of 0.15% and 0.6% by weight of cement (ACI 318). Investigations on SFRC specimens exposed to marine tidal cycles showed no corrosion of low-carbon steel and galvanized steel fibers embedded in the matrix at Cl^- concentration in excess of 2% (by weight of cement) (Mangat and Gurusamy 1987a, 1988). Melt extract fibers remained free from corrosion at much greater levels of chloride ion concentrations.

Currently, no standards exist that evaluate the corrosion resistance of SFRC. Mangat and Guruswamy (1987b) exposed 4 x 4 x 20 in. (100 x 100 x 500 mm) prisms to laboratory sea-water spray in a chamber that provided two wet cycles and two dry cycles in 24 hours. Similar specimens were also exposed to real tide action. In all cases, control specimens kept in the laboratory air or in water tanks were also prepared to allow for direct comparison. The studies have shown that low-carbon steel and galvanized steel fibers that are exposed at the concrete surface during casting are prone to corrosion under marine exposure. No such corrosion occurs in melt extract fibers, as they remain free from corrosion under prolonged marine exposure. The corrosion of fibers can be more intense if the concrete is cracked. Based on strength and toughness results, reported permissible crack widths have been as high as 0.006 in. (0.15 mm) and 0.008 in. (0.20 mm) for low carbon steel fibers and melt-extract fibers, respectively. Precracked specimens exposed to a coastal environment (Hannant and Edginton 1975) but remote from the tidal zone underwent significant carbonation. No corrosion was observed in fibers bridging cracks of widths less than 0.01 in. (0.25mm).

Standard tests to evaluate corrosion resistance of SFRC can be based on the determination of Cl^- concentration in concrete and carbonation. The long-term mechanical properties of SFRC, such as flexural strength and particularly toughness (based on load-deflection curves), provide suitable tests for the evaluation of corrosion in SFRC (Mangat and Guruswamy 1987b).

An extensive study of SFRC was undertaken to investigate the corrosion of individual fibers in cracked specimens (Nemegeer et al. 2003). The research was conducted to quantify

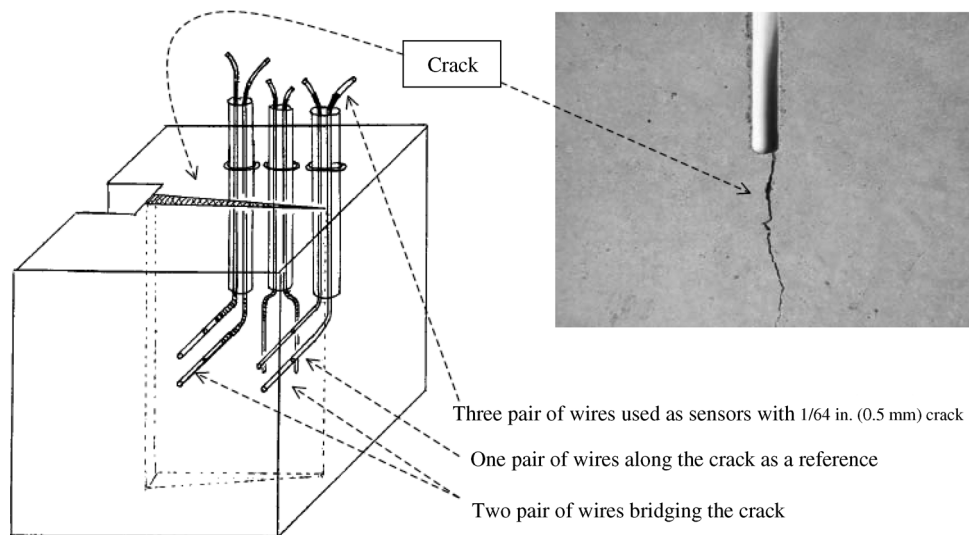


Fig. 4.5—Setup for the corrosion testing of FRC specimens.

Table 4.3—Summary of testing protocol

	1	2	3	4
First week	Outside exposure	Submerged in demi water	Submerged in demi water	Submerged in 5% NaCl
Second week	Outside exposure	Dried in lab atmosphere	Dried in CO ₂ atmosphere	Dried in CO ₂ atmosphere

the amount of corrosion and assess the durability of the fibers in a cracked situation. Notched cubes with dimensions 4 x 4 x 4 in. (100 x 100 x 100 mm) were cast containing 78 kg/m³ (131 lb/yd³) of hooked-end steel fibers. Both uncoated carbon steel and galvanized steel fibers were tested. The cubes were split to a predetermined crack width using a mechanical wedge usually used for the wedge splitting test. Two different crack widths were evaluated—0.008 in. (0.2 mm) and 0.02 in. (0.5 mm). Figure 4.5 represents the schematics of the setup used in these studies for the corrosion testing of specimens. Electrochemical testing is done on these precracked cubes in which fibers are embedded as sensors. The comparison is made between fibers bridging the cracks at different crack widths and fibers fully embedded in the concrete.

The electrochemical impedance for each sensor is measured at different time intervals to give an indication of the rate of corrosion. The resistivity of the concrete is also determined. The samples were exposed to four different environments: outside ambient, demineralized (demi) water + air, demineralized (demi) water + CO₂, and 5% NaCl + CO₂. Two-week-long cycles of exposure were used. The first environment represented samples that were subjected to continuous outside exposure. Table 4.3 shows how the cycles were carried out during the entire 18-month-long process conducted in 2-week rotations.

Microscopic analysis of the fibers afterward enabled the researchers to observe the different types of corrosion, the presence and nature of the corrosion products, and an estimate of the degree of corrosion (corrosion depth).

Mechanical performance was assessed using the wedge-splitting tests on the precracked cubes before exposure and after exposure to the various environments. The samples were exposed for 6, 12, or 18 months and then reloaded to assess any change in post-peak behavior. The study concluded that:

- Carbonation depth in all samples was small, from 0.04 to 0.08 in. (1 to 2 mm) even for specimens dried in the CO₂ environment. The type of concrete seemed to be the determining factor;
- Specimens wetted in NaCl environment were completely penetrated with chlorides: up to 0.048 oz Cl⁻/lb (3 g Cl⁻/kg) concrete;
- Independent of exposure conditions, no decrease in strength was observed after 18 months of exposure;
- Rusty fibers could be found in the noncracked concrete only directly at the surface, in the carbonated zone. Galvanized fibers at the surface showed no staining;
- Electrochemical measurements on sensors placed in the sound, noncarbonated concrete showed a comparably high electrochemical impedance, as did the sensors that bridged the crack. For all exposure conditions, except wetting in NaCl, this impedance was higher than 1 MΩ, indicating absolutely negligible corrosion. This corresponds with the microscopic analysis;
- Some sensors in the specimens wetted in the NaCl showed impedance lower than 1 MΩ. Microscopic analysis showed minor corrosion. Maximum measured corrosion depth after 18 months was locally 640 μm. (16 μm), but the overall reduction of the diameter was very small—less than 400 μm. (10 μm);
- Zinc-coated fibers showed a positive effect toward corrosion resistance; no staining at the surface and no corrosion of the steel was observed, although the zinc layer at some places had disappeared; and
- The crack width up to 0.02 in. (0.5 mm) seemed to have no adverse effect on corrosion (Bernard 2004b).

CHAPTER 5—APPLICATIONS AND DURABILITY-BASED DESIGN

5.1—Case studies of applications of FRC materials for durability

Rapid advances in FRC materials technology have enabled civil engineers to incorporate FRC in a variety of applications. These applications have resulted in improvements in safety, economy, and functionality of structures.

The enhanced properties of FRC depend on the contribution of constituents and affect the overall mechanical and durability response. In many areas, the durability of a structure can be significantly affected by the use of fiber reinforcement. Examples include aspects of plastic shrinkage cracking due to restrained shrinkage, which is a primary problem occurring in concrete structures with a relatively large surface area such as walls, bridge decks, slabs, and overlays. These applications are susceptible to rapid changes in temperature and humidity resulting in high water evaporation and high potential for shrinkage cracking. The addition of fibers is an effective method to control plastic shrinkage cracking. The following sections provide examples where the use of fiber reinforcement has resulted in enhanced performance of the structural system.

5.1.1 Thin bridge deck overlays—Fiber-reinforced concrete promises to provide a long-term solution to bridge deck problems (Krstulovic-Opara et al. 1995). Material characteristics of conventional SFRC and slurry-infiltrated high-performance steel fiber concrete are discussed. Several case studies are summarized to document the use of steel fibers in pavements and bridge deck overlays during the past three decades.

Zhang et al. (2002) present a methodology to use FRC as a ductile strip for durability enhancement of concrete slabs, proposing that cracking in plain concrete can be avoided due to the high strain capacity of engineered cementitious composite (ECC) materials.

5.1.2 Marine structures—Steel and macro-synthetic fiber-reinforced shotcrete has been used in Canada to repair marine structures in very severe climates. These marine structures in Canada are subject to aggressive environments including mechanical damage from ship impacts, exposure to strong currents laden with salt and abrasive sediments, alkali reactivity and, most significantly, between 200 to 300 freezing-and-thawing cycles per year. A number of projects have been undertaken over the past 20 years to repair marine structures (Gilbride 2002). All of these projects used shotcrete to repair deteriorating concrete. Both steel fiber and macrosynthetic FRC were used in the repairs. The success of these projects is demonstrated over a 10- to 20-year observation period. Condition surveys revealed that the repairs had excellent freezing-and-thawing resistance after exposure to over 2000 freezing and thawing cycles, excellent impact resistance, and a high degree of crack control.

5.1.3 Tunnel linings—Tunnels are usually designed with circular or semi-circular cross sections to take advantage of their inherent strength. The walls of tunnels, or tunnel linings, are designed to stabilize the inside surface of the tunnel and allow it to undergo slight movement so that the



Fig. 5.1—Channel Tunnel Rail Link tunnel lining made with SFRC.

natural ground on top can form an arch and carry vertical loads around the opening. Either sprayed concrete, shotcrete, or cast-in-place concrete is used to form the final lining of the tunnel. There are numerous cases reported of tunnel linings spalling from water infiltration and corrosion of the reinforcing bars. Reinforcement corrosion causes spalling of the concrete cover and further exposes the reinforcement to deterioration. Steel fiber concrete has been used in combination with, or as a replacement for, the temperature and shrinkage steel in tunnel linings. The use of the steel fibers alone eliminates the issue of concrete spalling because this phenomenon is not observed with steel fiber concrete. The use of discrete steel fibers does not provide a continuous water pathway as does continuous bar reinforcement. When used in combination with bar reinforcement, the onset of deterioration is significantly delayed. Steel fiber concrete has been used successfully in permanent sprayed and cast-in-place linings to reduce crack widths to less than 0.2 mm (0.01 in.) (Vandewalle 2005).

Between 2002 and 2004, a 13.2 mile (20 km) tunnel was constructed linking the Channel Tunnel Rail Link with downtown London, England. The tunnel is lined with precast concrete segments (Fig. 5.1). When segments are in the ground as a complete ring, the concrete is mostly in compression, and reinforcement is not needed. The segments, however, are under significant load during production, handling and erection, and from tunnel-boring machine shove forces. In subsurface applications, aggressive ground conditions can result in significant corrosion of conventional reinforcing bars that leads to concrete spalling. Steel fibers were selected to increase segment robustness during handling and eliminate the possibility of concrete spalling. The segments were designed as structural plain concrete, and steel fibers were added at a rate of 51 lb/yd³ (30 kg/m³). A nine-segment ring was chosen over a seven-segment ring to reduce the risk of inducing bending moments in steel fiber-reinforced segments. The tunnel has an inside diameter of 22 ft (6.9 m)

and the segments are 14 in. (350 mm) thick. In addition, micro-polymeric fibers were specified for fire protection. The polymeric fibers were added at a rate of 1.7 lb/yd³ (1 kg/m³) (Voigt et al. 2004).

CHAPTER 6—REFERENCES

6.1—Referenced standards and reports

The standards and reports listed below were the latest editions at the time this document was prepared. Because these documents are revised frequently, the reader is advised to contact the proper sponsoring group if it is desired to refer to the latest version.

American Association of State Highway Transportation Officials

PP34 Standard Practice for Cracking Tendency Using a Ring Specimen

American Concrete Institute

209R Prediction of Creep, Shrinkage, and Temperature Effects in Concrete Structures
 216.1/216.1M Code Requirements for Determining the Fire Endurance of Concrete and Masonry Construction Assemblies
 224.2R Cracking of Concrete Members in Direct Tension
 318/318M Building Code Requirements for Structural Concrete and Commentary
 544.1R Report on Fiber-Reinforced Concrete
 544.3R Guide for Specifying, Proportioning, and Production of Fiber-Reinforced Concrete
 549.2R Report on Thin Reinforced Cementitious Products

ASTM International

C666/C666M Standard Test Method for Resistance of Concrete to Rapid Freezing and Thawing
 C672/C672M Standard Test Methods for Scaling Resistance of Concrete Surfaces Exposed to Deicing Chemicals
 C1185 Standard Test Methods for Sampling and Testing Non-Asbestos Fiber-Cement Flat Sheet, Roofing and Siding Shingles, and Clapboards
 C1399 Standard Test Method for Obtaining Average Residual-Strength of Fiber-Reinforced Concrete
 C1550 Standard Test Method for Flexural Toughness of Fiber-Reinforced Concrete (Using Centrally Loaded Round Panel)
 C1579 Standard Test Method for Evaluating Plastic Shrinkage Cracking of Restrained Fiber-Reinforced Concrete (Using a Steel Form Insert)
 C1581/C1581M Standard Test Method for Determining Age at Cracking and Induced Tensile Stress Characteristics of Mortar and Concrete Under Restrained Shrinkage
 E119 Standard Test Methods for Fire Tests of Building Construction and Materials

These publications may be obtained from these organizations:

American Association of State Highway and Transportation Officials (AASHTO)
 444 N. Capitol St. NW, Suite 249
 Washington, DC 20001
 www.transportation.org

American Concrete Institute
 38800 Country Club Drive
 Farmington Hills, MI 48331
 www.concrete.org

ASTM International
 100 Barr Harbor Dr.
 West Conshohocken, PA 19428
 www.astm.org

6.2—Cited references

ACI Committee 209, 1982, "Prediction of Creep, Shrinkage, and Temperature Effects in Concrete Structures," *Designing for Creep and Shrinkage in Concrete Structures*, SP-76, American Concrete Institute, Farmington Hills, MI, pp. 193-300.

ACI Committee 222, 1985, "Corrosion of Metals in Concrete," *ACI Materials Journal*, V. 82, No. 1, Jan.-Feb., pp. 3-32.

Aindow, A. J.; Oakley, D. R.; and Proctor, B. A., 1984, "Comparison of the Weathering Behaviour of GRC with Predictions Made from Accelerated Aging Tests," *Cement and Concrete Research*, V. 14, No. 2, pp. 271-274.

Aldea, C. M.; Peled, A.; and Shah, S. P., 2000, "Permeability of Cracked High Performance Fiber Reinforced Cement Based Composites," *BEFIP 2000*, RILEM, Lyon, France.

Aldea, C. M.; Rapoport, J.; Shah S. P.; and Karr, A., 2001, "Combined Effect of Cracking and Water Permeability of Fiber-Reinforced Concrete: Concrete Under Severe Conditions," *Proceedings of the Third International Conference on Concrete Under Severe Conditions*, N. Banthia, K., Sakai, O. E. Gjörv, eds., Vancouver, BC, Canada, pp. 71-78.

Ali, F. A.; Connolly, R.; and Sullivan, P. J. E., 1997, "Spalling of High Strength Concrete at Elevated Temperatures," *Journal of Applied Fire Science*, V. 6, No. 1, pp. 3-14.

Allan, M. L., and Kukacha, L. E., 1995, "Strength and Durability of Polypropylene Grouts," *Cement and Concrete Research*, V. 25, No. 3, pp. 511-521.

Ambrose, J., and Péra, J., 2005, "Durability of Glass-Fibre Cement Composites: Comparison Between Normal, Portland and Calcium Sulphoaluminate Cements," *Proceedings Composites in Construction 2005—Third International Conference*, Lyon, France, pp. 1197-1204.

ASM International, 1988, "Engineering Plastics," *Engineered Materials Handbook*, V. 2, Metals Park, OH, 185 pp.

ASM International, 1990, "Properties and Selection: Irons, Steels and High Performance Alloys," *Metals Handbook*, tenth edition, V. 1, Materials Park, OH, p. 774.

Balaguru, P. N., and Kurtz, S., 2000, "Post-Crack Creep of Polymeric Fiber-Reinforced Concrete in Flexure," *Cement and Concrete Research*, V. 30, No. 2, pp. 183-190.

- Balaguru, P. N., and Ramakrishnan, V., 1986, "Freeze-Thaw Durability of Fiber-Reinforced Concrete," *ACI Materials Journal*, V. 83, No. 5, Sept.-Oct., pp. 374-382.
- Balaguru, P. N., and Shah, S. P., 1992, *Fiber-Reinforced Cement Composites*, McGraw Hill, Inc., New York, 530 pp.
- Ball, H. P., 2002, "Long Term Durability of Naturally Aged, GFRC Mixes Containing Forton Polymer," *2002 Proceedings of the 12th Congress of the GRCA*, J. N. Clarke and R. Ferry, eds., Dublin, Ireland, May, pp. 73-82.
- Ball, H. P., 2003, "Durability of Naturally Aged, GFRC Mixes Containing Forton Polymer and SEM Analysis of the Fracture Interface," *2003 Proceedings of 13th Congress of the GRCA*, J. N. Clarke and R. Ferry, eds., Barcelona, Spain, Oct.
- Banthia, N., and Gupta, R., 2006, "Influence of Polypropylene Fiber Geometry on Plastic Shrinkage Cracking in Concrete," *Cement and Concrete Research*, V. 36, No. 7, pp. 1263-1267.
- Banthia, N., and Yan, C., 2000, "Shrinkage Cracking in Polyolefin Fiber-Reinforced Concrete," *ACI Materials Journal*, V. 97, No. 4, July-Aug., pp. 432-437.
- Banthia, N.; Djeridane, S.; and Pigeon, M., 1992, "Electrical Resistivity of Carbon and Steel Micro-Fiber Reinforced Cements," *Cement and Concrete Research*, V. 22, No. 5, pp. 804-814.
- Banthia, N.; Yan, C.; and Mindess, S., 1996, "Restrained Shrinkage Cracking in Fiber-Reinforced Concrete: A Novel Test Technique," *Cement and Concrete Research*, V. 26, No. 1, pp. 9-14.
- Bayasi, M. Z., and Soroushian, P., 1992, "Effect of Steel Fiber-Reinforcement on Fresh Mix Properties of Concrete," *ACI Materials Journal*, V. 89, No. 4, July-Aug., pp. 369-374.
- Bažant, Z. P., and Najjar, L. J., 1971, "Drying of Concrete as a Nonlinear Diffusion Problem," *Cement Concrete Research*, V. 1, No. 5, pp. 461-473.
- Bažant, Z. P., and Panula, L., 1978, "Practical Prediction of Time-Dependent Deformations of Concrete," *Materials and Structures*, V. I-VI, No. 11, (1978), pp. 307-316, 317-328, 425-434, and No. 12, (1979) pp. 169-183.
- Bažant, Z. P.; Kim, J. K.; and Panula, L., 1991, "Improved Prediction Model for Time-Dependent Deformations of Concrete: Part 1—Shrinkage," *Materials and Structures*, V. 24, No.143, pp. 327-345.
- Beaupre, D., 1994, "Rheology of High Performance Shotcrete in Civil Engineering," University of British Columbia, Vancouver, BC, Canada, 249 pp.
- Beddows, J., and Purnell, P., 2003, "Durability of New Matrix Glass Fibre-Reinforced Concrete," *GFRC 2003 Proceedings of 12th Congress of the GRCA*, J. N. Clarke and R. Ferry eds., Barcelona, Spain, pp. 1-11.
- Bentur, A., 1986, "Mechanisms of Potential Embrittlement and Strength Loss of Glass Fiber-Reinforced Cement Composites," *Proceedings of Durability of Glass Fiber-Reinforced Concrete Symposium organized by PCI*, S. Diamond, ed., Chicago, pp. 109-123.
- Bentur, A., and Akers, S. A. S., 1989, "The Microstructure and Ageing of Cellulose Fibre-Reinforced Cement Composites Cured in a Normal Environment," *The International Journal of Cement Composites and Lightweight Concrete*, V. 11, No. 2, pp. 99-109.
- Bentur, A., and Diamond, S., 1984, "Fracture of Glass Fiber-Reinforced Cement," *Cement and Concrete Research*, V. 14, No. 1, pp. 31-34.
- Bentur, A., and Mindess, S., 1990, *Fiber-Reinforced Concrete*, Elsevier Science Publishing, Co, New York, 449 pp.
- Bentz, D. P., 2000, "Fibers, Percolation, and Spalling of High-Performance Concrete," *ACI Materials Journal*, V. 97, No. 3, May-June, pp. 351-359.
- Bergstrom, S. G., and Gram, H. E., 1984, "Durability of Alkali-Sensitive Fibres in Concrete," *The International Journal of Cement Composites and Lightweight Concrete*, V. 6, No. 2, pp. 75-80.
- Berke, N. S., and Dalliare, M. P., 1994, "The Effect of Low Addition Rate of Polypropylene Fibers on Plastic Shrinkage Cracking and Mechanical Properties of Concrete," *Fiber-Reinforced Concrete: Development and Innovations*, SP-142, J. I. Daniel and S. P. Shah, eds., American Concrete Institute, Farmington Hills, MI, pp. 19-41.
- Bernard, E. S., 2004a, "Creep of Cracked Fiber-Reinforced Shotcrete Panels" *Shotcrete: More Engineering Developments*, Taylor and Francis, London, pp. 47-57.
- Bernard, E. S., 2004b, "Durability of Fiber-Reinforced Shotcrete," *Shotcrete: More Engineering Developments*, Taylor and Francis, London, pp. 59-64.
- Bijen, J., 1983, "Durability of Some Glass Fiber-Reinforced Cement Composites," *ACI JOURNAL, Proceedings* V. 80, No. 4, July-Aug., pp. 304-311.
- Bijen, J., 1986, "A Survey of New Developments in Glass Composition, Coatings and Matrices to Extend Service Life of GFRC," *Proceedings—Durability of Glass Fiber-Reinforced Concrete Symposium organized by PCI*, S. Diamond, ed., Chicago, IL, pp. 251-269.
- Bijen, J., 1990, "Improved Mechanical Properties of Glass Fiber-Reinforced Cement by Polymer Modification," *Cement and Concrete Composites*, V. 12, No. 2, pp. 95-101.
- Bijen, J., and Jacobs, M. J. N., 1981, "Properties of Glass Fiber-Reinforced, Polymer Modified Cement," *Journal of Material and Structures*, V. 15, No. 89, pp. 445-452.
- Bilodeau, A.; Kodur, V. K. R.; and Hoff, G. C., 2004, "Optimization of the Type and Amount of Polypropylene Fibres for Preventing Spalling of Lightweight Concrete Subjected to Hydrocarbon Fire," *Cement and Concrete Composites*, V. 26, No. 2, pp. 163-174.
- Biryukovich, K. L., 1957, "Concrete with Fibre-Glass Reinforcement," Department of Scientific and Industrial Research, co-operative Russian Translation Scheme (Oct. 1958), *Stroitel'naya Promyshlennost*, V. 6, pp. 23-27.
- Biryukovich, K. L.; Biryukovich, Y. L.; and Biryukovich, D. L., 1965, "Glass Fiber-Reinforced Cement," published by Budivel'nik, Kiev, 1964, CERA Translation, No. 12, London.
- Biryukovich, K. L., and Biryukovich, Y. L., 1961, "Glass Fibre-Reinforced Cement, A Construction Material with Unstressed Glass Fibre," *Stroit Material*, V. 11, A-22, pp. 18-20.
- Bissonnette, B.; Therrien, Y.; Pleau, R.; Pigeon, M.; and Saucier, F., 2000, "Steel Fiber-Reinforced Concrete and

Multiple Cracking," *Canadian Journal of Civil Engineering*, V. 27, No. 4, pp. 774-784.

Bolander, J. E., 2004, "Numerical Modeling of Fiber-Reinforced Cement Composites: Linking Material Scales," *Proceedings of the Sixth International RILEM Symposium on Fibre-Reinforced Concretes—BEFIB 2004*, M. di Prisco, R. Felicetti, and G. A. Plizzari, eds., RILEM, pp. 45-60.

Bolander, J. E., and Berton, S., 2004, "Simulation of Shrinkage Induced Cracking in Cement Composite Overlays," *Cement and Concrete Composites*, V. 26, No. 7, pp. 861-871.

Bostrom, L., 2002, "The Performance of Some Self-Compacting Concrete when Exposed to Fire," *SP Report 23*, SP Swedish National Testing and Research Institute, 37 pp.

Brameshuber, W., and Brockmann, T., 2001a, "Calcium Aluminate Cement as Binder for Textile Reinforced Concrete," *International Conference on Calcium Aluminate Cements (CAC)*, Edinburgh, Scotland, pp. 659-666.

Brameshuber, W., and Brockmann, T., 2001b, "Development and Optimization of Cementitious Matrices for Textile Reinforced Concrete," *2002 Proceedings of the 12th Congress of the GRCA*, N. Clarke and R. Ferry, eds., Dublin, Ireland, pp. 237-249.

Bui, V. K.; Geiker, M. R.; and Shah, S. P., 2003, "Rheology of Fiber-Reinforced Cementitious Materials," *International Workshop on High Performance Fiber-Reinforced Cement Composites*, Ann Arbor, MI, pp. 221-231.

Canovas M. F.; Kaviche, G. M.; and Selva, N. H., 1990, "Possible Ways of Preventing Deterioration of Vegetable Fibres in Cement Mortars, Vegetable Plants and Their Fibres as Building Materials," *Proceedings of the Second International RILEM Symposium*, Chapman & Hall, pp. 120-129.

Canovas, M. F.; Selva, N. H.; and Kawiche, G. M., 1992, "New Economical Solutions for Improvement of Durability of Portland Cement Mortars Reinforced with Sisal Fibers," *Materials and Structures*, V. 25, No. 7, pp. 417-422.

Cantin, R., and Pigeon, M., 1996, "Deicer Salt Scaling Resistance of Steel Fiber -Reinforced Concrete," *Cement and Concrete Research*, V. 26, No. 11, pp. 1639-1648.

Chandra, S.; Berntsson, L.; and Anderberg, Y., 1980, "Some Effects of Polymer Addition on the Fire Resistance of Concrete," *Cement and Concrete Research*, V. 10, No. 3, pp. 367-375.

Christensen, B. J.; Coverdale, R. T.; Olson, R. A.; Ford, S. J.; Garboczi, E. J.; Jennings, H. M.; and Mason, T. O., 1994, "Impedance Spectroscopy of Hydrating Cement Pastes," *Journal of the American Ceramic Society*, V. 77, No. 11, pp. 2789-2804.

Cook, D. J., and Uher, C., 1973, "The Thermal Conductivity of Fiber-Reinforced Concrete," *Cement and Concrete Research*, V. 4, No. 174, pp. 497-509.

Coussot, P., 1993, "Rheologie des Boues et Laves Torren-tielles—Études de Dispersions et Suspensions Concentrees," L'Institut National Polytechnique de Grenoble, et Etudes du Cemagref, 418 pp.

Craig, R., 2004, "Dartford Cable Tunnel," *Tunneling & Trenchless Construction*, pp. 17-19.

Craig, R., 2006, "Malmö's Construction Starts," *Tunnelling & Trenchless Construction*, pp. 12-14.

Cuypers, H.; Gu, J.; Croes, K.; Dumortier, S.; and Wastiels, J., 2000, "Evaluation of Fatigue and Durability Properties of E-Glass Fiber-Reinforced Phosphate Cementitious Composite," *Proceedings, Brittle Matrix Composites 6*, A. M. Brandt, V. C. Li, and I. H. Marshall, eds., Warsaw, Poland, pp. 127-136.

Cuypers, H.; Van Itterbeeck, P.; De Bolster, E.; and Wastiels, J., 2005, "Durability of Cementitious Composites," *Proceedings, Composites in Construction 2005—Third International Conference*, Lyon, France, pp. 1205-1212.

Cuypers, H.; Wastiels, J.; Orłowsky, J.; and Raupach, M., 2003, "Measurement of the Durability of Glass Fibre-Reinforced Concrete and Influence of Matrix Alkalinity," *Proceedings of Brittle Matrix Composites 7*, A. M. Brandt, V. V. Li, and I. H. Marshall, eds., Warsaw, Poland, pp. 163-172.

Cuypers, H.; Wastiels, J.; Van Itterbeeck, P.; De Bolster, E.; Orłowsky, J.; and Raupach, M., 2006, "Durability of Glass Fibre-Reinforced Composites Experimental Methods and Results," *Composites Part A*, V. 37, No. 2, pp. 207-215.

Dehn, F., and König, G., 2003, "Fire Resistance of Different Fiber-Reinforced High-Performance Concretes," *High Performance Fiber-Reinforced Cement Composites 4*, A. E. Naaman and H. W. Reinhardt, eds., RILEM, pp. 189-204.

di Prisco, M.; Felicetti, R.; Gambarova, P. G.; and Failla, C., 2003, "On the Fire Behavior of SFRC and SFRC Structures in Tension and Bending," *High Performance Fiber-Reinforced Cement Composites 4*, A. E. Naaman and H. W. Reinhardt, eds., RILEM, pp. 205-220.

Douglas, J. F., and Garboczi, E. J., 1995, "Intrinsic Viscosity and the Polarizability of Particles Having a Wide Range of Shapes," *Advances in Chemical Physics*, S. A. Rice, ed., V. 91, John Wiley & Sons, New York, pp. 85-153.

England, G. L., and Khoylou, N., 1995, "Moisture Flow in Concrete Under Steady State Non-Uniform Temperature States: Experimental Observations and Theoretical Modeling," *Nuclear Engineering and Design*, V. 156, pp. 83-107.

Ferrara, L., 2003, "The Use of Viscosity-Enhancing Admixtures to Improve Homogeneity of Fibre Distribution in Steel Fibre-Reinforced Concretes," *Proceedings of the 7th International Symposium on Brittle Matrix Composites*, ZTUREK RSI and Woodhead Publishing, Warsaw, Poland, pp. 287-300.

Forgeron, D., and Trottier, J. F., 2004, "Evaluating the Effects of Combined Freezing and Thawing and Flexural Fatigue Loading Cycles on the Fracture Properties of FRC," *High-Performance Structures and Materials II, The Built Environment*, V. 76, pp. 177-188.

Gambarova, P. G., 2004, "Overview of Recent Advancements in FRC Knowledge and Applications with Specific Reference to High Temperature," *Proceedings, RILEM Technical Meeting*, pp. 125-140.

Garboczi, E.; Snyder, K.; Douglas, J.; and Thorpe, M., 1995, "Geometrical Percolation Threshold of Overlapping Ellipsoids," *Physical Review*, E 52, pp. 819-828.

Garrett, R., 2004, "Construction Chemistry at Weehawken," *Tunnelling & Trenchless Construction*, pp. 21-25.

Gartshore, G. C.; Kempster, E.; and Tallentire, A. G., 1991, "A New High Durability Cement for GRC Products,"

Proceedings, *The Glass Fibre- Reinforced Cement Association 6th Biennial Congress*, pp. 3-12.

Giaccio, G.; Giovambattista, A.; and Zerbino, R., 1986, "Concrete Reinforced with Collated Steel Fibers: Influence of Separation," *ACI JOURNAL, Proceedings V. 83, No. 2, Mar.-Apr.*, pp. 232-235.

Gilbride, P.; Morgan, D. R.; and Bremner, T. W., 2002 "Deterioration and Rehabilitation of Berth Faces in Tidal Zones at the Port of Saint John," *Shotcrete, V. 4, No. 4, Fall*, pp. 32-38.

Goldfein, S., 1963, "Plastic Fibrous-Reinforcement for Portland Cement," *Technical Report No. 1757-TR, U.S. Army Engineering Research and Development Laboratories, Fort Belvoir, VA*, 16 pp.

Gram, H. E., 1983, "Durability of Natural Fibres in Concrete," *S-100 44, No. 1:83, Swedish Cement and Concrete Research Institute, Stockholm*, 255 pp.

Gram, H. E., 1988, "Durability of Natural Fibres in Concrete," *Natural Fibre-Reinforced Cement and Concrete*, R. Swamy, ed., pp. 143-172.

Gu, P.; Xie, P.; Beaudoin, J. J.; and Brosseau, R., 1992a, "AC Impedance Spectroscopy I: A New Equivalent Circuit Model for Hydrated Portland Cement Paste," *Cement and Concrete Research, V. 22*, pp. 833-840.

Gu, P.; Xie, P.; Beaudoin, J. J.; and Brosseau, R., 1992b, "AC Impedance Spectroscopy II: Microstructural Characterization of Hydrating Cement-Silica Fume Systems," *Cement and Concrete Research, V. 23*, pp. 157-168.

Guimarães, S. S., 1990, "Vegetable Fiber Cement Composites," *Vegetable Plants and Their Fibres as Building Materials*, Proceedings of the Second International RILEM Symposium, H. S. Sobral, ed., Chapman & Hall, pp. 98-107.

Hammond, E., and Robson, T. D., 1955, "Comparison of Electrical Properties of Various Cements and Concretes," *The Engineer, V. 199, No. 5156*, pp. 78-80 and 114-115.

Hannant, D. J., 1978, *Fibre Cements and Fibre Concretes*, John Wiley & Sons, Chichester, England, 95 pp.

Hannant, D. J., and Edginton, J., 1975, "Durability of Steel Fiber-Reinforced Concrete," *RILEM Symposium on Fiber-Reinforced Cement and Concrete*, Construction Press, Lancaster, V. 1, pp. 159-169.

Hoff, G. C., 1987, "Durability of Fiber Reinforced Concrete in a Severe Marine Environment," *Concrete Durability: Katharine and Bryant Mather International Conference, SP-100*, J. M. Scanlon, ed., American Concrete Institute, Farmington Hills, MI, pp. 997-1041.

Hoff, G. C., 1996, "Fire Resistance of High-Strength Concretes for Offshore Concrete Platforms," *Performance of Concrete in Marine Environment*, Proceedings of the Third CANMET/ACI International Conference, SP-163, American Concrete Institute, Farmington Hills, MI, pp. 53-87.

Holt, E., 2003, "Self-Compacting Concrete: State-of-the-Art. Part IV: Fire Resistance," *Report RTE40-1R-15/2003*, Finland, 14 pp.

Hossain, A. B., and Weiss, W. J., 2004, "Assessing Residual Stress Development and Stress Relaxation in Restrained Concrete Ring Specimens," *Cement and Concrete Composites, V. 26, No. 5*, pp. 531-540.

Hossain, A. B.; Pease, B.; and Weiss, W. J., 2003, "Quantifying Restrained Shrinkage Cracking Potential in Concrete Using the Restrained Ring Test with Acoustic Emission," *Transportation Research Record, Concrete Materials and Construction 1834*, pp. 24-33.

Hu, C.; de Lallard, F.; Sedran, T.; Boulay, C.; Bosc, F.; and Deflorenne, F., 1996, "Validation of BTRHEOM, the New Rheometer for Soft-to-Fluid Concrete," *Materials and Structures, V. 29*, pp. 620-631.

Hughes, B., and Fattuhi, N., 1976, "Workability of Steel Fiber Reinforced Concrete," *Magazine of Concrete Research, V. 28, No. 96*, pp. 157-161.

Ishida, H.; Iwase, H.; Rokugo, K.; and Kayanagi, W., 1985, "Improvement of Freezing and Thawing Resistance of Lightweight Concrete by Steel Fiber Addition," *Transactions of Japan Concrete Institute, V. 7*, pp. 135-140.

John, V. M.; Agopyan, V.; and Derolle, A., 1990, "Durability of Blast-Furnace-Slag-Based Cement Mortar Reinforced with Coir Fibres," *Vegetable Plants and Their Fibres as Building Materials*, Proceedings of the Second International RILEM Symposium, Chapman & Hall, pp. 87-97.

John, V. M.; Cincotto, M. A.; Sjostrom, C.; Agopyan, V.; and Oliveira, C. T. A., 2005, "Durability of Slag Mortar Reinforced with Coconut Fibre," *Cement and Concrete Composites, V. 27*, pp. 565-574.

Kalifa, P.; Menneteau, F. D.; and Quenard, D., 2000, "Spalling and Pore Pressure in HPC at High Temperatures," *Cement and Concrete Research, V. 30*, pp. 1915-1927.

Kim, P. J.; Wu, H. C.; Lin, Z.; Li, V. C.; deLhoneux, B.; and Akers, S. A. S., 1999, "Micromechanics-Based Durability Study of Cellulose Cement in Flexure," *Cement and Concrete Research, V. 29*, pp. 201-208.

Kobayashi, K., 1983, "Development of Fiber-Reinforced Concrete in Japan," *International Journal of Cement Composites, V. 5*, pp. 27-40.

Krstulovic-Opara, N.; Haghayeghi, A. R.; Haidar, M.; and Krauss, P. D., 1995, "Use of Conventional and High-Performance Steel Fiber-Reinforced Concrete for Bridge Deck Overlays," *ACI Materials Journal, V. 92, No. 6, Nov.-Dec.*, pp. 669-677.

Kuder, K., and Shah, S. P., 2003, "Effects of Pressure on Resistance to Freezing and Thawing of Fiber-Reinforced Cement Board," *ACI Materials Journal, V. 100, No. 6, Nov.-Dec.*, pp. 463-468.

Kuder, K., and Shah, S. P., 2004, "Freeze-Thaw Durability of Commercial Fiber-Reinforced Cement Board," *Thin Reinforced Cement-Based Products and Construction Systems, SP-224*, A. Dubey, ed., American Concrete Institute, Farmington Hills, MI, pp. 145-159.

Kuder, K.; Özyurt, N.; Mu, B.; and Shah, S. P., 2004, "The Rheology of Fiber-Reinforced Cement Paste Evaluated by a Parallel Plate Rheometer," *Advances in Concrete through Science and Engineering*, Northwestern University, Evanston, IL, USA: International Union of Laboratories and Experts in Construction Materials (RILEM).

Kumar, A., and Roy, D. M., 1985, "Microstructure of Glass Fiber/Cement Paste Interface in Admixture Blended Portland Cement Samples," *Proceedings, Durability of*

Glass Fiber-Reinforced Concrete Symposium organized by PCI, S. Diamond, ed., Chicago, pp. 147-156.

Kurarray, 2007, "PVA Fibers and Industrial Materials," *Applications: Asbestos Replacement*, <http://www.kurarray-am.com/pvaf/asbestos.php> (accessed Dec. 16, 2009).

Lakkad, S. C.; Miatt, B. B.; and Parson, B., 1972, "The Thermal Conductivity of a Statistically Isotropic Heterogeneous Medium," *Journal of Physics D: Applied Physics*, V. 5, pp. 1304-1320.

Lawler, J. S.; Zampini, D.; and Shah, S. P., 2002, "Permeability of Cracked Hybrid Fiber Reinforced Mortar Under Load," *ACI Materials Journal*, V. 99, No. 4, July-Aug. pp. 379-392.

Leonard, S. and Bentur, A., 1984, "Improvement of the Durability of Glass Fiber-Reinforced Cement Using Blended Cement Matrix," *Cement and Concrete Research*, V. 14, pp. 717-728.

Li, Z.; Mobasher, B.; and Shah, S. P., 1990, "Effect of Aging on the Interfacial Properties of GFRC," *Proceedings, Materials Research Society, MRS Fall Meeting, Boston, MA*, V. 211, pp. 113-118.

Litherland, K. L., 1986, "Test Methods for Evaluating the Long Term Behaviour of Glass Fibre-Reinforced Concrete," *Proceedings of the Durability of Glass Fiber-Reinforced Concrete Symposium organized by PCI*, S. Diamond, ed., Chicago, pp. 210-221.

Litherland, K. L., and Proctor, B. A., 1986, "The Effect of Matrix Formulation, Fibre Content and Fibre Composition on the Durability of Glass Fibre-Reinforced Cement," *Proceedings of the Durability of Glass Fiber Reinforced Concrete Symposium organized by PCI*, S. Diamond, ed., Chicago, pp. 124-135.

Litherland, K. L.; Oakley, D. R.; and Proctor, B. A., 1981, "The Use of Accelerated Aging Procedures to Predict the Long-Term Strength of GRC Composites," *Cement and Concrete Research*, V. 11, pp. 455-466.

Ludirdja, D.; Berger, R. L.; and Young, J. F., 1989, "Simple Method for Measuring Water Permeability of Concrete," *ACI Materials Journal*, V. 86, No. 5, Sept.-Oct., pp. 433-439.

Ma, Y.; Tan, M.; and Wu, K., 2002, "Effect Of Different Geometric Polypropylene Fibers on Plastic Shrinkage Cracking of Cement Mortars," *Materials and Structures*, V. 35, No. 247, pp. 165-169.

Mackay, J., and Trottier, J. F., 2004, "Post-Crack Behavior of Steel and Synthetic FRC under Flexural Creep," *Proceedings of the Second International Conference on Engineering Developments in Shotcrete*, Cairns, Australia, pp. 183-192.

Majumdar, A. J., and Laws, V., 1991, *Glass Fibre-Reinforced Cement*, Oxford BSP Professional Books, 197 pp.

Malek, R. I. A., and Roy, D. M., 1991, "Modeling the Rheological Behavior of Cement Pastes: A Review," *Advances in Cementitious Materials Ceramic Transactions*, American Ceramic Society, Westerville, OH, pp. 31-40.

Mane, S. A.; Desai, T. K.; Kingsbury, D.; and Mobasher, B., 2002, "Modeling of Restrained Shrinkage Cracking in Concrete Materials," *Concrete: Material Science to Application—A Tribute to S. P. Shah*, SP-206, P. Balaguru, A. Naaman, and

W. Weiss, eds., American Concrete Institute, Farmington Hills, MI, pp. 219-242.

Mangat, P. S., and Gurusamy, K., 1987a, "Chloride Diffusion in Steel Fiber-Reinforced Marine Concrete," *Cement and Concrete Research*, V. 17, pp. 385-396.

Mangat, P. S., and Gurusamy, K., 1987b, "Permissible Crack Widths in Steel Fiber-Reinforced Marine Concrete," *Materials and Structures*, V. 20, pp. 338-347.

Mangat, P. S., and Gurusamy, K., 1987c, "Long-Term Properties of Steel Fiber-Reinforced Marine Concrete," *Materials and Structures*, V. 20, No.118, pp. 273-282.

Mangat, P. S., and Gurusamy, K., 1988, "Corrosion Resistance of Steel Fibers in Concrete Under Marine Exposure," *Cement and Concrete Research*, V. 18, pp. 44-54.

Mangat, P. S., and Swamy, R., 1974, "Compactibility of Steel Fiber-Reinforced Concrete," *Concrete*, V. 8, No. 5, pp. 34-35.

Marikunte, S.; Aldea, C.; and Shah, S., 1997, "Durability of Glass Fiber-Reinforced Cement Composites: Effect of Silica Fume and Metakaolin," *Journal of Advanced Cement Based Composites*, V. 5, pp. 100-108.

Martinola, G., and Wittmann, F. H., 1995, "Application of Fracture Mechanics to Optimize Repair Mortar Systems," *Fracture Mechanics of Concrete Structures*, F. H. Wittmann, ed., pp. 1481-1486.

McCarter, W. J., 1996, "The AC Impedance Response of Concrete During Early Hydration," *Journal of Materials Science*, V. 31, pp. 6285-6292.

McCarter, W. J., and Brosseau, R., 1990, "The AC Response of Hardened Cement Paste," *Cement and Concrete Research*, V. 20, pp. 891-900.

Mindess, S.; Young, J. F.; and Darwin, D., 2003, *Concrete*, second edition, Prentice Hall, Upper Saddle River, NJ, 644 pp.

Mobasher, B., 2000, *Modeling of Toughness Degradation and Embrittlement in Cement-Based Composite Materials Due to Interfacial Aging*, ASCE Engineering Mechanics Division Conference, Baltimore, MD. (CD-ROM)

Mobasher, B., and Shah, S. P., 1989, "Test Parameters in Toughness Evaluation of Glass Fiber-Reinforced Concrete Panels," *ACI Materials Journal*, V. 86, No. 5, Sept.-Oct., pp. 448-458.

Mohr, B. J.; Nanko, H.; and Kurtis, K. E., 2005a, "Durability of Kraft Pulp Fiber-Cement Composites to Wet/Dry Cycling," *Cement and Concrete Composites*, V. 27, pp. 435-448.

Mohr, B. J.; Nanko, H.; and Kurtis, K. E., 2005b, "Durability of Thermomechanical Pulp Fiber-Cement Composites to Wet/Dry Cycling," *Cement and Concrete Research*, V. 35, pp. 1646-1649.

Mohr, B. J.; Biernacki, J. J.; and Kurtis, K. E., 2006, "Microstructural and Chemical Effects of Wet/Dry Cycling on Pulp Fiber-Cement Composites," *Cement and Concrete Research*, V. 36, pp. 1240-1251.

Monfore, G. E., 1968, "The Electrical Resistivity of Concrete," *Journal of the PCA Research and Development Laboratories*, V. 10, No. 2, pp. 35-48.

Moody, G.; Vondran, G.; and Hoff, G., 2003, "Fiber-Reinforced Concrete (FRC) for Fire Resistance," *Proceedings*

SP of Session on High Performance Fiber-Reinforced Cementitious Composites for Increased Blast & Impact Resistance, Vancouver, BC, Canada, 18 pp.

Morel, K. C., 1970, "The Thermal Conductivity of Steel Fiber Reinforced Concrete Mortar," Master of Science Thesis, Clarkson University, Potsdam, NY, Aug.

Naaman, A. E.; Wongtanakitcharoen, T.; and Hauser, G., 2005, "Influence of Different Fibers on Plastic Shrinkage Cracking of Concrete," *ACI Materials Journal*, V. 102, No. 1, Jan.-Feb., pp. 49-58.

Najm, H., and Balaguru, P., 2002, "Effect of Large-Diameter Polymeric Fibers on Shrinkage Cracking of Cement Composites," *ACI Materials Journal*, V. 99, No. 4, July-Aug., pp. 345-351.

Nawy, E. G., 1996, *Fundamentals of High Strength High Performance Concrete*, Longman Group, UK, 360 pp.

Nemegeer, D.; Vanbrabant, J.; and Stang, H., 2003, "Brite-Euram Program on Steel Fibre Concrete, Durability Corrosion Resistance of Cracked Fibre-Reinforced Concrete," *Test and Design Methods for Steel Fibre Reinforced Concrete-Background and Experiences*, B. Schnütgen and L. Vandewalle, eds., RILEM Technical Committee 162, TDF Workshop, Proceedings Pro 31, pp. 47-66.

Niemuth, M., 2004, "Using Impedance Spectroscopy to Detect Flaws in Concrete," MSCE thesis, Purdue University, West Lafayette, IN, 117 pp.

Orlowsky, J.; Raupach, M.; Cuypers, H.; and Wastiels, J., 2005, "Durability Modeling of Glass Fiber Reinforcement in Cementitious Environment," *Materials and Structures*, V. 38, pp. 155-162.

Özyurt, N.; Mason, T. O.; and Shah, S. P., 2006a, "Correlation of Fiber Dispersion, Rheology and Mechanical Performance," *16th European Conference on Fracture: Measuring, Monitoring and Modeling Concrete Properties: In Honor of Surendra P. Shah*, Alexandroupolis, Greece.

Özyurt, N.; Mason, T. O.; and Shah, S. P., 2006b, "Non-Destructive Monitoring of Fiber Orientation using AC-IS: An Industrial Scale Application," *Cement and Concrete Research*, V. 36, No. 9, pp. 1653-1660.

Özyurt, N.; Mason, T. O.; and Shah, S. P., 2007, "Correlation of Fiber Dispersion, Rheology and Mechanical Performance of FRCs," *Cement and Concrete Composites*, V. 29, No. 2, pp. 70-79.

Özyurt, N.; Woo, L. Y.; Mason, T. O.; and Shah, S. P., 2006, "Monitoring Fiber Dispersion in FRCs: Comparison of AC-Impedance Spectroscopy and Image Analysis," *ACI Materials Journal*, V. 103, No. 5, Sept.-Oct., pp. 340-347.

Özyurt, N.; Woo, L. Y.; Mu, B.; Shah, S. P.; and Mason, T. O., 2004, "Detection of Fiber Dispersion in Fresh and Hardened Cement Composites," *Advances in Concrete Through Science and Engineering, An International Symposium during the RILEM Spring Meeting*, Northwestern University, Evanston, IL.

PCI Committee on Glass Fiber-Reinforced Concrete Panels, 1981, "Recommended Practice for Glass Fiber-Reinforced Concrete Panels," *Journal of the Prestressed Concrete Institute*, V. 26, No. 1, pp. 25-93.

"PCI Recommended Practice for Glass Fiber-Reinforced Concrete Panels," 2002, MNL128-01, fourth edition, Prestressed Concrete Institute, Jan., 104 pp.

Peled, A.; Torrents, J. M.; Mason, T. O.; Shah, S. P.; and Garboczi, E. J., 2001, "Electrical Impedance Spectra to Monitor Damage During Tensile Loading of Cement Composites," *ACI Materials Journal*, V. 98, No. 4, July-Aug., pp. 313-322.

Picandet, V.; Khelidj, A.; and Bastian, G., 2001, "Effect of Axial Compressive Damage on Gas Permeability of Ordinary and High-Performance Concrete," *Cement and Concrete Research*, V. 31, No. 11, pp. 1525-1532.

Proctor, B. A.; Oakley, D. R.; and Litherland, K. L., 1982, "Developments in the Assessment and Performance of GRC Over 10 years," *Composites*, V. 13, pp. 173-179.

Purnell, P., and Beddows, J., 2005, "Durability and Simulated Ageing of New Matrix Glass Fiber-Reinforced Concrete," *Cement and Concrete Composites*, V. 27, Issues 9-10, pp. 875-884.

Purnell, P.; Short, N. R.; Page, C. L.; Majumdar, A. J.; and Walton, P. L., 1999, "Accelerated Aging Characteristics of Glass-Fiber Reinforced Cement Made with New Cementitious Matrices," *Composites A*, V. 30, pp. 1073-1080.

Qi, C., and Tianyou, B., 2003, "A Review of the Development of the GRC Industry in China," *2003 Proceedings of the 13th Congress of the GRCA*, J. N. Clarke and R. Ferry, eds., Barcelona, Spain, Paper 37. (CD-ROM)

Qi, C., and Weiss, J., 2003, "Characterization of Plastic Shrinkage Cracking in Fiber-Reinforced Concrete Using Image Analysis and a Modified Weibull Function," *Materials and Structures*, V. 35, No. 6, pp. 386-395.

Qi, C.; Weiss, W. J.; and Olek, J., 2003, "Characterization of Plastic Shrinkage Cracking in Fiber Reinforced Concrete Using Semi-Automated Image Analysis," *Concrete Science and Engineering*, V. 36, No. 260, pp. 386-395.

Qi, C.; Weiss, W. J.; and Wang, H., 2006, "Quantifying the Impact of Plastic Shrinkage Cracking in the Corrosion of Reinforced Concrete to Improve Service Life Prediction," *6th ISCC and CANMET ACI International Symposium on Concrete Technology for Sustainable Development*, Xi'an, China, pp. 1325-1335.

Radlinska, A.; Moon, J.-H.; Rajabipour, F.; and Weiss, W. J., 2006, *The Ring Test: History and Developments*, O. Jensen, P. Lura, and K. Kovler, eds., pp. 205-214.

Ramakrishna, G., and Sundararajan, T., 2004, "Studies on the Durability of Natural Fibres and the Effect of Corroded Fibres on the Strength of Mortar," *Cement and Concrete Composites*, V. 27, No. 5, May, pp. 575-582.

Ramakrishnan, V., and Coyle, W. V., 1986, "Steel Fiber-Reinforced Superplasticized Concretes for Rehabilitation of Bridge Decks and Highway Pavements," *Report No. DOT-RSPA-DMA-50/84/2*, U.S. Dept. of Transportation, Office of University Research, Washington, DC, p. 158.

Ramakrishnan, V.; Brandshaug, T.; Coyle, W.; and Schrader, E., 1980, "Comparative Evaluation of Concrete Reinforced with Straight Steel Fibers and Fibers with Ends Glued Together into Bundles," *ACI JOURNAL, Proceedings* V. 77, No. 3, Mar., pp. 135-143.

- Rapoport, J. R., and Shah, S. P., 2005, "Cast-in-Place Cellulose Fiber-Reinforced Cement Paste, Mortar, and Concrete," *ACI Materials Journal*, V. 102, No. 5, Sept.-Oct., pp. 299-306.
- Rapoport, J.; Aldea, C.; Shah, S. P.; Ankenman, B.; and Karr, A., 2002, "Permeability of Steel Fiber Reinforced Concrete," *Journal of Materials in Civil Engineering*, ASCE, V. 14, No. 4, pp. 355-358.
- Reza, F.; Batson, G. B.; Yamamuro J. A.; and Lee, J. S., 2001, "Volume Electrical Resistivity of Carbon Fiber Cement Composites," *ACI Materials Journal*, V. 98, No. 1, Jan.-Feb., pp. 25-35.
- Reza, F.; Batson, G. B.; Yamamuro, J. A.; and Lee, J. S., 2003, "Resistance Changes During Compression of Carbon Fiber-Cement Composites," *Journal of Materials in Civil Engineering*, ASCE, V. 15, No. 5, pp. 476-483.
- Reza, F.; Yamamuro, J. A.; and Batson, G. B., 2004, "Electrical Resistance Changes in Compact Tension Specimens of Carbon Fiber Cement Composites," *Cement and Concrete Composites*, V. 26, pp. 873-881.
- Rider, R. G., and Heidersbach, R. H., 1980, "Degradation of Metal Fiber-Reinforced Concrete Exposed to a Marine Environment," *STP 713, Corrosion of Reinforcing Steel in Concrete*, ASTM International, West Conshohocken, PA, pp. 75-92.
- Saechtling, H., 1987, *International Plastics Handbook*, Hanser Gardner Publications, 644 pp.
- Sanjuán, M. A.; Andrade, C.; and Bentur, A., 1997, "Effect of Crack Control in Mortars Containing Polypropylene Fibers on the Corrosion of Steel in a Cementitious Matrix," *ACI Materials Journal*, V. 94, No. 2, Mar.-Apr., pp. 134-141.
- Sant, G.; Lura, P.; and Weiss, W. J., 2006, "A Discussion of Analysis Approaches for Determining 'Time-Zero' from Chemical Shrinkage and Autogenous Strain Measurements In Cement Paste," *Conference on Concrete Curing*, O. Jensen, P. Lura, and K. Kovler, eds., Lyngby, Denmark, pp. 375-384.
- Savastano, H.; Warden, P. G.; and Coutts, R. S. P., 2001, "Ground Blast-Furnace Slag as a Matrix for Cellulose-Cement Materials," *Cement and Concrete Composites*, V. 23, pp. 389-397.
- Schneider, U., 1983, "Behavior of Concrete at High Temperatures," RILEM, Committee 44-PHT.
- Schupack, M., 1985, "Durability of SFRC Exposed to Severe Environments," *Proceedings, Steel-Fiber Concrete, US-Sweden Joint Seminar (NSF-STU)*, Stockholm, June 3-5, pp. 479-496.
- Schwein, R., 1988, "Elevated Temperature Study of Fiber-mesh Polypropylene Fiber-Reinforced Concrete," Schwein/Christensen Engineering Ltd., Project No. 87248, Feb.
- Shah, H. R., and Weiss, W. J., 2006, "Quantifying Shrinkage Cracking in Fiber-Reinforced Concrete Using the Ring Test," *Materials and Structures*, V. 39, No. 9, pp. 887-899.
- Shah, S. P.; Ludirdja, D.; Daniel J. I.; and Mobasher, B., 1988, "Toughness-Durability of Glass Fiber-Reinforced Concrete Systems," *ACI Materials Journal*, V. 91, No. 5, Sept-Oct., pp. 352-360, and discussion, V. 92, No. 4, *ACI Materials Journal*, July-Aug. 1989, p. 425.
- Shah, S. P.; Ouyang, C.; Marikunte, S.; Yang, W.; and Becq-Giraudon, E., 1998, "A Method to Predict Shrinkage Cracking of Concrete," *ACI Materials Journal*, V. 95, No. 4, July-Aug., pp. 339-346.
- Silva, F. A.; Melo Filho, J. A.; Toledo Filho, R. D.; and Fairbairn, E. M. R., 2006a, "Mechanical Behavior and Durability of Compression Moulded Sisal Fiber-Cement Mortar Laminates (SFCML)," *Proceedings of the 1st International RILEM Symposium on Textile Reinforced Concrete*, pp. 171-180.
- Silva, F. A.; Toledo Filho, R. D.; Fairbairn, E. M. R., 2006b, "Accelerated Aging Characteristics of Sisal Fiber-Cement Based Composites Made with a CH Free Cementitious Matrix," *Brazilian Conference Non-Conventional Materials and Technologies in Ecological and Sustainable Construction*, Brazil, Nocmat, V. 1. pp. 2869-2878.
- Sim, J.; Park, C.; and Moon, D. Y., 2005, "Characteristics of Basalt Fiber as a Strengthening Material for Concrete Structures," *Composite Part B: Engineering*, V. 36, pp. 504-512.
- Soroushian, P., and Marikunte S., 1992, "Long-Term Durability and Moisture Sensitivity of Cellulose Fiber-Reinforced Cement Composites," *Fibre-Reinforced Cement and Concrete*, R. N. Swamy, ed., E&FN Spon, London, pp. 1166-1184.
- Struble, L. J.; Puri, U.; and Ji, X., 2001, "Concrete Rheometer," *Advances in Cement Research*, V. 13, No. 2, pp. 53-63.
- Swamy, R. N., and Mangat, P., 1974, "Influence of Fiber Geometry on the Properties of Steel Fiber-Reinforced Concrete," *Cement and Concrete Research*, V. 4, No. 3, pp. 451-465.
- Swamy, R. N., and Stavarides, H., 1979, "Influence of Fiber Reinforcement on Restrained Shrinkage Cracking," *ACI JOURNAL, Proceedings* V. 76, No. 3, May-June, pp. 443-460.
- Tan, K. H.; Paramasivam, P.; and Tan, K. C., 1994, "Instantaneous and Long-Term Deflections of Steel Fiber-Reinforced Concrete Beams," *ACI Structural Journal*, V. 91, No. 4, July-Aug., pp. 384-393.
- Tatnall, P. C., 2002, "Shotcrete in Fires: Effects of Fibers on Explosive Spalling," *Shotcrete*, V. 4, No. 4, pp. 10-12.
- Tattersall, G. H., 1991, *The Workability and Quality Control of Concrete*, E&FN Spon, 262 pp.
- Tattersall, G. H., and Bloomer, S. J., 1979, "Further Development of the Two-Point Test for Workability and Extension of Its Range," *Magazine of Concrete Research*, pp. 202-210.
- Thompson, N. E., 1968, "A Note on the Difficulties of Measuring the Thermal Conductivity of Concrete," *Magazine of Concrete Research*, V. 29, No. 62, p. 46.
- Toledo Filho, R. D.; Ghavami, K.; England, G. L.; and Scrivener, K., 2000a, "Durability of Sisal Fibre-Reinforced Mortar Composites," *Proceedings of the Fifth International RILEM Symposium*, P. Rossi and G. Chanvillard, eds., pp. 655-664.
- Toledo Filho, R. D.; Scrivener, K.; England, G. L.; and Ghavami, K., 2000b, "Durability of Alkali-Sensitive Sisal and Coconut Fibers in Cement Mortar Composites," *Cement and Concrete Composites*, V. 22, pp. 127-143.
- Toledo Filho, R. D.; Ghavami, K.; England, G. L.; and Scrivener, K., 2003, "Development of Vegetable Fiber-

Mortar Composites of Improved Durability," *Cement and Concrete Composites*, V. 25, pp. 185-196.

Torrents, J. M.; Mason, T. O.; and Garboczi, E. J., 2000, "Impedance Spectra of Fiber-Reinforced Cement-Based Composites: A Modeling Approach," *Cement and Concrete Research*, V. 30, pp. 585-592.

Torrents, J. M.; Mason, T. O.; Peled, A.; Shah, S. P.; and Garboczi, E. J., 2001, "Analysis of Impedance Spectra of Short Conductive Fiber Reinforced Composites," *Journal of Material Science*, V. 36, No. 16, pp. 4003-4012.

Trottier, J. F., and Forgeron, D., 2001, "Cumulative Effects of Flexural Fatigue Loading and Freezing and Thawing Cycles on the Flexural Toughness of Fiber Reinforced Concrete," *Third International Conference on Concrete Under Severe Conditions: Environment and Loading*, Vancouver, BC, Canada, V. 1, pp. 1165-1176.

Trottier, J. F.; Morgan, D.; Forgeron, D.; and Cantin, R., 1996, "Durabilité et Performance Mécanique de Bétons Renforcés de Fibres," 2^e Colloque International sur les Bétons Renforcés de Fibres Métalliques, Toulouse.

Troxell, G. E.; Davis, H.; and Kelly, J., 1968, *Composition and Properties of Concrete*, McGraw-Hill, 334 pp.

Troxell, G. E.; Raphael, J. M.; and Davis, R. E., 1958, "Long-Time Creep and Shrinkage Tests of Plain and Reinforced Concrete," *Proceedings of the American Society for Testing and Materials*, V. 58, pp. 1101-1120.

Tsukamoto, M., and Wörner, J.-D., 1991, "Permeability of Cracked Fibre-Reinforced Concrete," *Darmstadt Concrete*, V. 6, pp. 123-135.

Ulm, F. J.; Acker, P.; and Levy, M., 1999, "The Chunnel Fire II: Analysis of Concrete Damage," *Journal of Engineering Mechanics*, V. 125, No. 3, pp. 283-289.

Vandewalle, M., 2005, *Tunneling is an Art*, NV Bekaert, SA, p 160.

Velasco, R. V.; Toledo Filho, R. D.; Fairbairn, E. M. R.; Lima, P. R. L.; and Neumann, R., 2004, "Spalling and Stress-Strain Behaviour of Polypropylene Fibre-Reinforced HPC After Exposure to High Temperatures," *6th RILEM Symposium on Fibre-Reinforced Concretes (BEFIB 2004)*, M. di Prisco, R. Felicetti, and G. A. Plizzari, eds., RILEM, pp. 699-708.

Voigt, T.; Bui, V. K.; and Shah, S. P., 2004, "Drying Shrinkage of Concrete Reinforced with Fibers and Welded-

Wire Fabric," *ACI Materials Journal*, V. 101, No. 3, May-June, pp. 233-241.

Vondran, G. L., 1987, "Making More Durable Concrete with Polymeric Fibers" *Concrete Durability: Katharine and Bryant Mather International Conference*, SP-100, J. M. Scanlon, ed., American Concrete Institute, Farmington Hills, MI, 382 pp.

Vondran, G. L., 1989, "Polypropylene FRC in Steel Deck Composite Slabs, ASCE Metal Deck," *Structural Materials, Proceedings of Structures Congress 1989*, J. F. Orofino, ed., ASCE, 10 pp.

Wallevik, O. H., and GjØrv, O. E., 1990, "Development of Coaxial Cylinder Viscometer for Fresh Concrete," *Properties of Concrete, RILEM Colloquium*, Hanover: Chapman and Hall, pp. 213-224.

Wang, K.; Jansen, D. C.; Shah, S. P.; and Karr, A. F., 1997, "Permeability Study of Cracked Concrete," *Cement and Concrete Research*, V. 27, No. 3, pp. 381-393.

Wongtanakitcharoen, T., and Namaan, A. E., 2007, "Unrestrained Early Age Shrinkage of Concrete with Polypropylene, PVA, and Carbon Fibers," *Materials and Structures*; V. 40, No. 3, pp. 289-300.

Woo, L. Y.; Wansom, S.; Özyurt, N.; Mu, B.; Shah, S. P.; and Mason, T. O., 2005, "Characterizing Fiber Dispersion in Cement Composites using AC-Impedance Spectroscopy," *Cement and Concrete Composites*, V. 27, No. 6, pp. 627-636.

Young, C. H., and Chern, J. C., 1991, "Practical Prediction Model For Shrinkage of Steel Fiber-Reinforced Concrete," *Materials and Structures*, V. 24, No. 141, pp. 191-201.

Zhang, J., and Li, V. C., 2001, "Influences of Fibers on the Drying Shrinkage of Fiber-Reinforced Cementitious Composite," *Journal of Engineering Mechanics*, ASCE, V. 127, No. 1, pp. 37-44.

Zhang, J.; Li, V. C.; Nowak, A.; and Wang, S., 2002, "Introducing Ductile Strip for Durability Enhancement of Concrete Slabs," *Journal of Materials in Civil Engineering*, ASCE, V. 14, No. 3, pp. 253-261.

Zhu, W., and Bartos, P. J. M., 1997, "Assessment of Interfacial Microstructure and Bond Properties in Aged GRC Using a Novel Microindentation Method," *Cement and Concrete Research*, V. 27, No. 11, pp. 1701-1711.



American Concrete Institute®
Advancing concrete knowledge

As ACI begins its second century of advancing concrete knowledge, its original chartered purpose remains “to provide a comradeship in finding the best ways to do concrete work of all kinds and in spreading knowledge.” In keeping with this purpose, ACI supports the following activities:

- Technical committees that produce consensus reports, guides, specifications, and codes.
- Spring and fall conventions to facilitate the work of its committees.
- Educational seminars that disseminate reliable information on concrete.
- Certification programs for personnel employed within the concrete industry.
- Student programs such as scholarships, internships, and competitions.
- Sponsoring and co-sponsoring international conferences and symposia.
- Formal coordination with several international concrete related societies.
- Periodicals: the *ACI Structural Journal* and the *ACI Materials Journal*, and *Concrete International*.

Benefits of membership include a subscription to *Concrete International* and to an ACI Journal. ACI members receive discounts of up to 40% on all ACI products and services, including documents, seminars and convention registration fees.

As a member of ACI, you join thousands of practitioners and professionals worldwide who share a commitment to maintain the highest industry standards for concrete technology, construction, and practices. In addition, ACI chapters provide opportunities for interaction of professionals and practitioners at a local level.

American Concrete Institute
38800 Country Club Drive
Farmington Hills, MI 48331
U.S.A.

Phone: 248-848-3700

Fax: 248-848-3701

www.concrete.org

Report on the Physical Properties and Durability of Fiber-Reinforced Concrete

The AMERICAN CONCRETE INSTITUTE

was founded in 1904 as a nonprofit membership organization dedicated to public service and representing the user interest in the field of concrete. ACI gathers and distributes information on the improvement of design, construction and maintenance of concrete products and structures. The work of ACI is conducted by individual ACI members and through volunteer committees composed of both members and non-members.

The committees, as well as ACI as a whole, operate under a consensus format, which assures all participants the right to have their views considered. Committee activities include the development of building codes and specifications; analysis of research and development results; presentation of construction and repair techniques; and education.

Individuals interested in the activities of ACI are encouraged to become a member. There are no educational or employment requirements. ACI's membership is composed of engineers, architects, scientists, contractors, educators, and representatives from a variety of companies and organizations.

Members are encouraged to participate in committee activities that relate to their specific areas of interest. For more information, contact ACI.

www.concrete.org



American Concrete Institute®
Advancing concrete knowledge